UCRL-2393
Unclassified-Physics Distribution

UNIVERSITY OF CALIFORNIA
Radiation Laboratory
Contract No. W-7405-eng-48

PRODUCTION OF H^3 AND He^3 IN HIGH-ENERGY DEUTERON-DEUTERON COLLISIONS

Charles S. Godfrey
(Thesis)

November 2, 1953

Berkeley, California

DISCLAIMER

UNITED STATES ATOMIC ENERGY COMMISSION

UCRL-2393

PRODUCTION OF H^3 AND He^3 IN HIGH-ENERGY DEUTERON-DEUTERON COLLISIONS (thesis)

By
Charles S. Godfrey

November 2, 1953

Radiation Laboratory
University of California, Berkeley

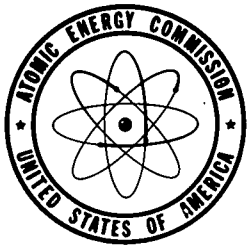

Technical Information Service, Oak Ridge, Tennessee

Subject Category, PHYSICS
Work performed under Contract No. W-7405-eng-48.

Printed in USA, Price 55 cents. Available from the Office of Technical Services, Department of Commerce, Washington 25, D. C.

AEC, Oak Ridge, Tenn.-W40482

PRODUCTION OF H^3 AND He^3 IN HIGH-ENERGY DEUTERON-DEUTERON COLLISIONS

Charles S. Godfrey

Radiation Laboratory, Department of Physics
University of California, Berkeley, California

November 2, 1953

ABSTRACT

The differential cross section for the process $d + d \rightarrow H^3 + p$ has been measured at six angles extending from 20° to 85° in the center-of-mass system. Deuterons of 190 Mev from the Berkeley 184-inch synchrocyclotron were used. A coincidence counting system, consisting of scintillation counters for both particles, was employed. Time of flight and range of the particles were used, both in identifying the process and in discriminating against background. The resulting cross section is highly peaked in the forward direction. The behavior is explained qualitatively by a theoretical calculation based on an extension of the stripping mechanism first proposed by Serber. The total cross section for the reaction is estimated to be 4.1 millibarns.

The relative production of H^3 from the above process and of He^3 from the process $d + d \rightarrow He^3 + n$ has been measured at 30° center-of-mass. The method of detection required that the particles traverse a magnetic channel and a pulse-height counter telescope. The pulses were displayed on a fast cathode-ray oscilloscope and recorded photographically. A liquid-deuterium target was employed. The comparison shows a ratio of H^3 to He^3 of 0.86 ± 0.14. These data support the hypothesis that charge symmetry of nuclear forces exists at high energy.

PRODUCTION OF H^3 AND He^3 IN HIGH-ENERGY DEUTERON-DEUTERON COLLISIONS

Charles S. Godfrey

Radiation Laboratory, Department of Physics
University of California, Berkeley, California

November 2, 1953

INTRODUCTION

When high-energy deuterons in the Berkeley 184-inch synchrocyclotron were first allowed to strike a target, it was found that an intense cone of high-energy neutrons was projected in the same direction of motion as the incident deuterons. Serber[1] proposed a "stripping" mechanism to explain its formation. In this process, one nucleon of the deuteron interacts suddenly with the target nucleus while the other nucleon is largely unaffected in its motion. It was felt that the formation of H^3 and He^3 particles in deuteron-deuteron collisions might be considered as a stripping process in which the neutron or proton, of one deuteron might interact with and "stick to" the other deuteron - leaving its partner to continue with essentially the same momentum it had at the instant of stripping. A theoretical calculation by Drs. Heckrotte and Bludman[2] makes it possible to predict the shape of the angular distribution for a pure stripping process.

The production of H^3 and He^3 in deuteron-deuteron collisions has been studied extensively by investigators using up to 10-Mev deuterons.[3, 4, 5, 6, 7, 8] The fact that the cross sections for these particles are essentially equal (except where Coulomb forces predominate) has been considered as evidence that charge symmetry exists up to these energies. The term "charge symmetry" is used herein to denote the equality of n - n nuclear forces to p - p forces of the same angular momentum and spin state, neglecting effects due to Coulomb forces and mass differences between the particles. Many other data have been published which confirm this conclusion. Ajzenberg and Lauritsen[9] conclude from their studies of nuclear spectroscopy that charge symmetry of nuclear forces, insofar as it is manifested in low-lying energy states, can be regarded as an

established fact. A study of the three-body stable nuclei[10] leads to the conclusion that the binding energies of H^3 and He^3 can be understood most simply under the assumption that charge symmetry exists for the ^1S state. Further evidence of charge symmetry can be inferred from low-energy scattering data,[11,12] which indicate that the dineutron is probably just unbound and that the assumption of equal scattering lengths for n - n and p - p scattering in the ^1S state is not inconsistent with these data.

Evidence of charge symmetry at high energies, where many higher states, strong tensor forces and meson fields are expected to play important roles, is very meager. Yet all theoretical approaches to high-energy scattering assume its existence. The most conclusive evidence would of course be a comparison of high-energy p - p scattering with n - n scattering. Since targets of neutrons do not exist, however, one must turn to less direct methods. Evidence is available in a comparison of n - d and p - d scattering at the same energy. The width of available neutron spectrums, however, and the differences of experimental technique required to perform the experiments, make a direct comparison of results difficult. A comparison of the results of Stern[13] for d - p scattering and those of Powell[14] and Youtz[15] for n - d scattering shows discrepancies in shape and absolute value that make any conclusion suspect. Barkas and Wilson[16] have examined the ratio for the production of π^+ and π^- mesons at 90° when carbon is bombarded with 390-Mev alpha particles. The mesons, however, are relatively low in energy and are appreciably affected by the Coulomb barrier. They conclude that the data are not inconsistent with the assumption of charge symmetry. A direct comparison of the production of H^3 and He^3 in 190-Mev deuteron-deuteron collisions can be made. The assumption of charge symmetry would require that these two cross sections be equal.

This experiment was designed to measure the absolute differential cross section for the process $d + d \rightarrow H^3 + p$ over as wide a range of angles as possible using 190-Mev deuterons. The data obtained could then be compared with those expected of a stripping process. Secondly, it was proposed to compare at one production angle the relative yields of H^3 and He^3. These data could serve as an argument for or against the assumption of charge symmetry at high energy.

GENERAL EXPERIMENTAL METHOD

Differential Cross Section for $d + d \rightarrow H^3 + p$

Since the external deuteron beam is essentially monoenergetic, the kinematics of the above process can be calculated uniquely for any scattering angle by applying the laws of conservation of energy and momentum. This calculation was carried out relativistically as outlined in Appendix B of reference 17. The results are summarized in Fig. 1. In theory one has only to place detectors at the proper correlated angles corresponding to any desired scattering angle and count the simultaneous creations of a H^3 and a proton by means of a coincidence circuit. Knowing the geometry involved, the particle flux, and the number of target particles, one can calculate the cross section by the well-known formula. Note that the calculation of kinematics has been carried out only for the range 0° to 90° center-of-mass. Since the colliding deuterons are indistinguishable, the cross section must be symmetric about 90° center-of-mass. It is necessary to measure the scattering only from 0° to 90° to obtain the complete differential cross section.

The high background in the Berkeley "cave" has been one of the major difficulties to be overcome for any low-cross-section experiment. Recently, time-of-flight techniques have been used successfully in the cave to reduce the effect of this background.[17] The range of energies and angles shown in Fig. 1 seemed quite suitable for the application of similar methods in the above process. Since the time of flight of the tritons over an eleven-foot path (the usable length of the cave) from target to detector was of the order of 30 millimicroseconds, it was necessary to use a coincidence circuit considerably faster than this. The circuit used had a resolving time of about 3 millimicroseconds.

As a further aid in discriminating against background and providing identification, absorbers were used in front of the detectors. These absorbers were calculated ideally to allow the desired particle to just stop at the back of the detector. Thus, heavily ionizing particles would generally not get through the absorber while lightly ionizing particles would give small pulses that could be biased out if they provided accidental coincidences.

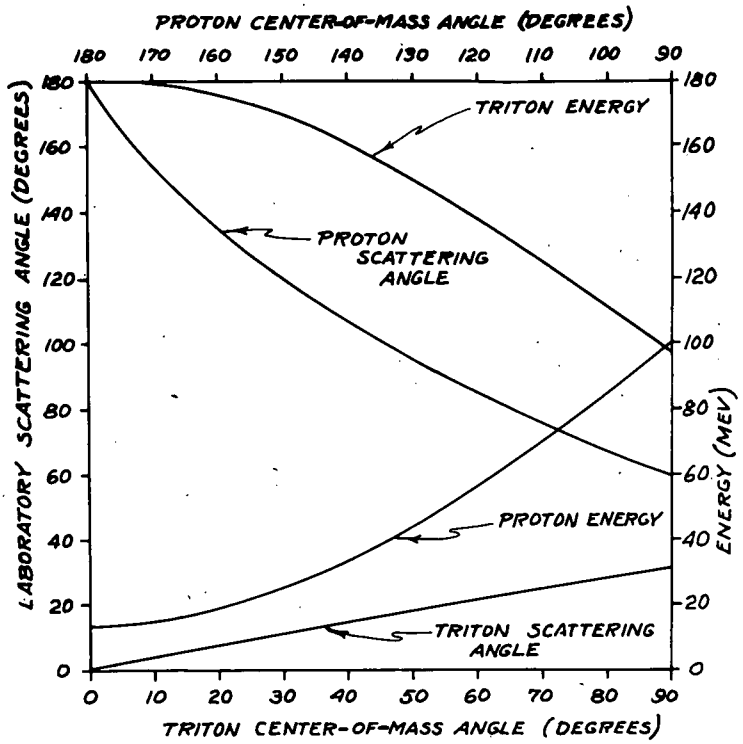

Fig. 1—Correlated angles and energies in the laboratory system for the process $d + d \rightarrow H^3 + p$ for scattering of the H^3 from 0° to 90° center-of-mass. Incident deuteron energy is 190 Mev.

The general experimental method consisted, therefore, in requiring a coincidence of triton and proton at the proper correlated angle, and requiring further that the particles have the proper time of flight and the proper range.

Comparison of H^3 and He^3 Production

In this case it was not feasible to use coincidence methods, since the neutron partner of the He^3 cannot be detected with any well defined efficiency. The first possibility explored was that of using pulse-height techniques for the single H^3 or He^3 with the added feature of time of flight to discriminate against background particles having different velocities from theirs. As first attempted, the single particle provided a pulse in a detector eleven feet from the target. This pulse served as one input to a coincidence circuit while a pulse corresponding to the beam at the target, suitably delayed to give proper time of flight, provided the other input. The resolving time for coincidence could not be less than the duration of the beam pulse, in this case approximately 10 millimicroseconds. Since the difference in the time of flight between the desired particle and the main flux of fast-particle background was about 10 millimicroseconds, it can be seen that time-of-flight techniques could not be very effective in discriminating against background. On a trial of this arrangement, it was found that the flux of particles hitting the detector and making coincidence with the beam pulse was so heavy that identification of particles by pulse-height techniques alone would be extremely tedious, if possible at all.

It was decided, therefore, to employ a magnetic channel and pulse height to provide the necessary separation and identification of the particles. In order to provide a direct comparison of H^3 and He^3, it was necessary to insure the same angular resolution, the same energy resolution and the same multiple-scattering efficiency for both particles. For a given scattering angle, both H^3 and He^3 will have essentially the same energy (about one Mev difference due to their mass difference). Originating in the same target, however, and passing through identical amounts of intervening windows in going from target to detector, they will have different scattering and energy distributions. The general scheme of attack had three basic features:

(1) The same magnetic channel (physically) was used for both particles at any given scattering angle. To detect He^3, the magnetic field intensity was reduced to half that used for H^3. This procedure had the advantage of insuring identical geometry for both particles.

(2) The average energy and the energy spread of the H^3 were made equal to those of the He^3. Any loss of counting efficiency due to energy spread was thereby balanced out.

(3) Multiple scattering was made to occur as near the target as possible. No restrictive openings or slits were used between the target and the entrance to the magnetic channel. For a process having an isotropic cross section, the particle flux at the entrance to the magnetic channel would simulate the light flux from a frosted light bulb, i.e., the number of particles per unit solid angle would be independent of the multiple scattering. The effect of multiple scattering would then be merely to spread out the energy spectrum and angular distribution of the particles entering the channel. Actually the cross section did vary slowly as a function of angle, but the geometry was such as to make this correction negligible. To still further minimize multiple scattering errors, the H^3 particles were made to pass through enough additional absorber to make their multiple scattering approximately equal to that of the He^3.

A pulse-height telescope behind the magnet provided pulses corresponding to specific ionization dE/dx and total energy (E). It may seem that the three parameters--Hρ, dE/dx, and E--overdetermine the separation problem. The separation of deuterons from tritons, however, is marginal under optimum conditions when only two parameters are used. It was felt that wider limits on the resolutions of both the magnetic channel and the pulse-height equipment could be allowed by the use of all three parameters.

Pulses from the dE/dx and E detectors were used to drive a fast double-coincidence circuit with a resolving time of 3 millimicroseconds. The resulting output was used to trigger an oscilloscope which then displayed both the dE/dx and E pulses on its screen. A continuously moving film recorded these pulses for later analysis. The fast-resolution circuit was used to cut

down the rate of accidental coincidences. In order to insure an efficiency of 100 percent for the counting of desired pulses, the oscilloscope trigger bias was set considerably below the level at which these pulses occurred. This meant that many low-energy pulses appeared on the film, but could be discriminated against by analyzing the pulse heights.

The general experimental method for comparing H^3 and He^3 production consisted in equalizing their energy spectrums, in reducing the effects of multiple scattering to a minimum, in requiring the particles to traverse a magnetic channel, and in recording the pulse heights given off by them in going through a thin detector and stopping at a thick detector.

DETAILED EXPERIMENTAL METHOD

Differential Cross Section for $d + d \rightarrow H^3 + p$

Apparatus

The experimental arrangement for a typical scattering angle is shown in Fig. 2. The incident 190-Mev deuterons were collimated to a beam 2 inches in diameter. The beam was monitored by an ionization chamber; ion current was integrated on a calibrated condenser and recorded in volts by a recording potentiometer. The calibration of the monitor for 190-Mev deuterons was performed by Dr. W. Crandall's group. The beam energy has been found by Stern[13] to be 192 ± 2 Mev. The targets of deuterated paraffin $(CD_2)_n$, polyethylene $(CH_2)_n$, and carbon (C) had diameters of 3 inches and had the same numbers of carbon atoms. A comparison of counting rates using $(CH_2)_n$ and C was used to make sure that no d - p process was contributing to the counting rate. The particle detector at the triton angle consisted of two trans-stilbene phosphors; each phosphor was 2 in. by 4 in. and was viewed by two 1P21 photomultiplier tubes. The phosphor thicknesses were selected so that the expected tritons, after having passed through suitable absorber, would lose 20 to 30 Mev in each phosphor. The two signals from a given phosphor were shaped by clipping to a width of 3 millimicroseconds and were added together. Trans-stilbene phosphors were used because their rise time is of the order of millimicroseconds; thus not so much of the pulse energy is lost by shaping as would be with some other commonly used phosphors. Figure 3 shows this shaper-adder-limiter circuit together with the last dynode of the photomultiplier.

The particle detector at the proton angle consisted of one trans-stilbene phosphor 1-1/2 in. by 3 in. and was viewed by two 1P21 photomultiplier tubes. The phosphor thickness was selected so that the expected protons, after suitable absorber, would lose about 20 Mev. The signals from the two photomultipliers were shaped and added as above and delayed by the length of coaxial cable calculated to match the expected triton signal time of arrival at the coincidence circuit. The two triton signals and the delayed proton signal were fed into a germanium diode triple-coincidence circuit having a resolution time of about 3 millimicroseconds with these pulses. Figure 4 is a schematic diagram of the

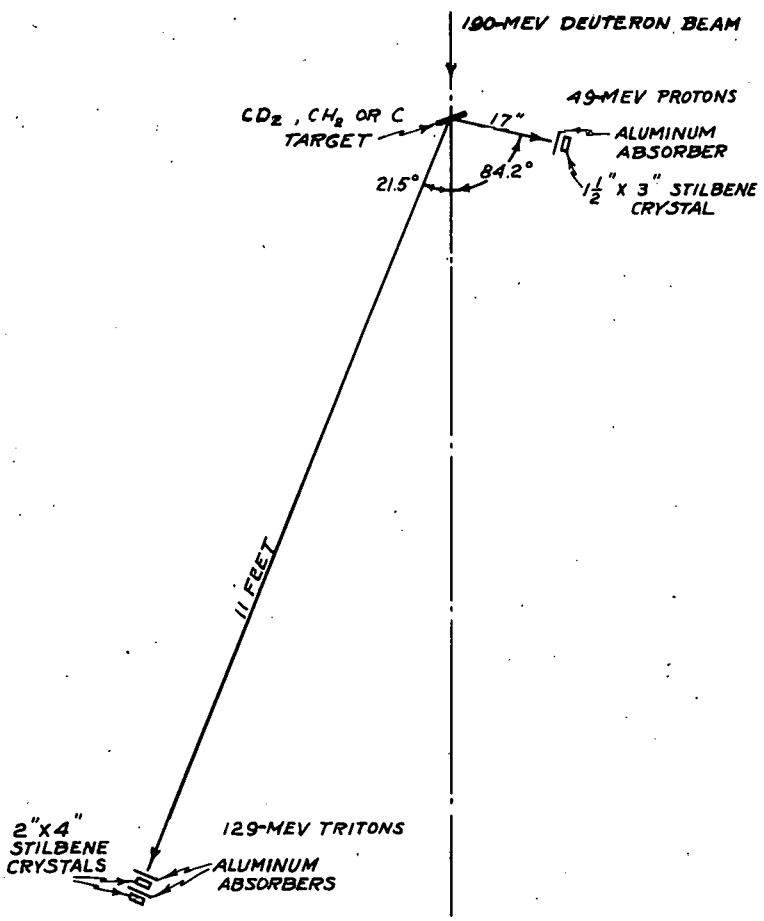

Fig. 2—Experimental arrangement for observing the process $d + d \rightarrow H^3 + p$.

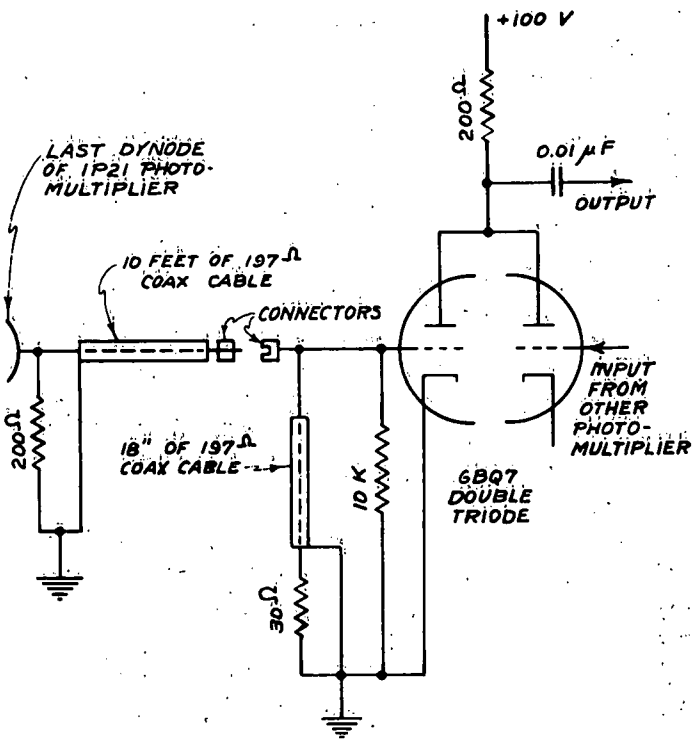

Fig. 3—Circuit used to shape, limit, and add photomultiplier pulses.

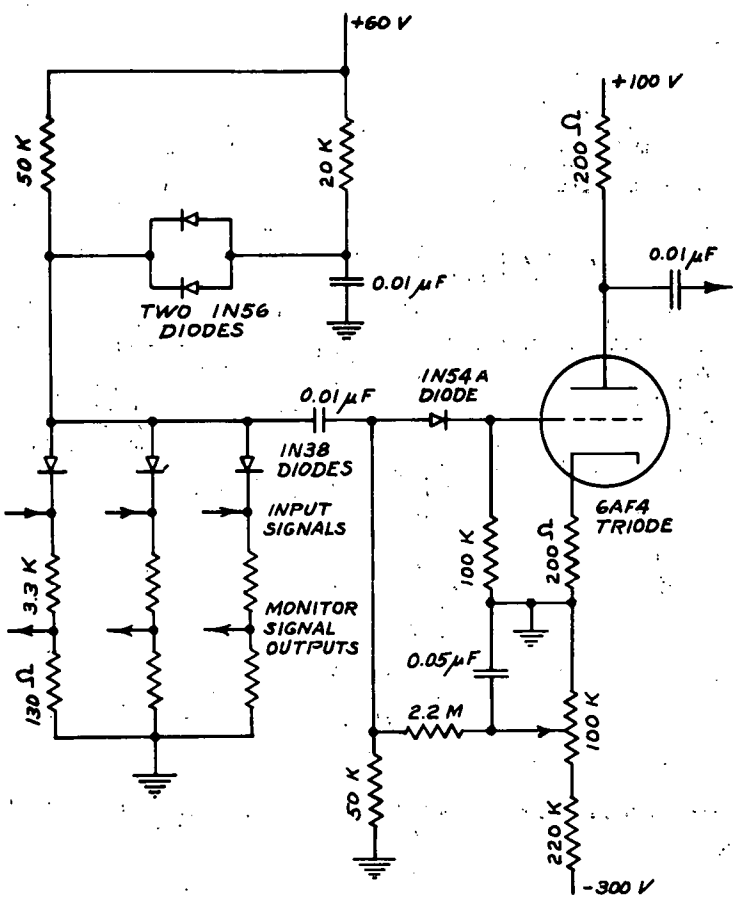

Fig. 4—Germanium diode triple-coincidence circuit.

coincidence circuit. The IN38 germanium diode inputs were used instead of tubes to increase the circuit sensitivity and eliminate the necessity for amplifiers between the detectors and the coincidence circuit. The two parallel IN56 diodes and associated components are due to Garwin.[18] They increase the discrimination ratio by clamping the output voltage except when all three input diodes are simultaneously cut off.

The IN54A diode in the grid of the output tube was introduced to increase further the discrimination of the circuit. A typical ratio of triple-to double-coincidence output pulse heights is around 25. The output signal of the coincidence circuit was amplified and recorded on two scaling counters with different bias settings. This procedure provided a check that one was operating on a bias plateau. The efficiency of similar counting equipment has been measured to be very nearly 100 percent. A more detailed account of the electronic equipment is being published by Dr. Richard Madey, who was the leader in its development.

Method

During the first run on the cyclotron, it was necessary to make sure that the process $d + d \rightarrow H^3 + p$ was really being observed. The identification consisted in (1) moving the triton counter horizontally and vertically out of its proper position, (2) changing the delay of the proton pulse from the proper calculated value, and (3) adding just enough absorber in front of the detectors to stop the expected particles. In each case the net counting rate should vanish.

The first step during a run was to make sure the detectors were operating on a voltage plateau. The net counting rate was plotted as a function of detector voltage and a voltage was chosen which lay on a flat portion of the curve. Next the net counting rate was measured as a function of beam intensity to make sure that the contribution of accidental coincidences was negligible. The differential cross section for the various scattering angles was then measured. In order to illustrate the detailed use of the time-of-flight technique and to show how it discriminates against background, a specific example is used:

For tritons scattering at a center-of-mass angle of 60°, the correlated laboratory angles are 21.5° for the triton and 84.2° for the proton. The geometry is shown in Fig. 2. Suppose a time origin is taken

when a pulse of deuterons passes through the target. These pulses have an approximate half-width of 10 millimicroseconds and are spaced 100 millimicroseconds apart. The triton-proton pair is created simultaneously, but any background pairs that might lead to accidental coincidences are created separately, spaced at most by the dimensions of the envelope of the beam pulse. The triton velocity is 0.30 c (c is the velocity of light), and the triton arrives at its counter in 38 millimicroseconds. The proton velocity is 0.31 c and the proton arrives at its counter in 5 millimicroseconds. Since the deuterons in the beam are bunched, they produce background, such as elastically scattered deuterons or inelastically scattered deuterons and protons that are also bunched. Each bunch tends to have a characteristic velocity. Protons characteristic of p - p scattering, for example, have a velocity of about 0.40 c. Over the 11 feet from target to detectors, the probability envelopes of the tritons and these protons are separated by about 11 millimicroseconds; since the resolving time of the coincidence unit is about 3 millimicroseconds, it is apparent that background from p - p scattering does not interfere with the counting of real events.

The time sequence is illustrated in Fig. 5. Delaying the proton signal by 33 millimicroseconds places the real triton-proton counts in coincidence. The locations in time of several possible sources of background are shown. Since the proton detector is close to the target, the proton-detector background is well separated from the triton-detector background, and possible accidental coincidences are reduced.

At this same scattering angle the absorbers used were such that any background particle had to traverse the equivalent of 5 g/cm^2 of aluminum before entering the back triton detector. This absorber stops protons of 70 Mev or less. Figure 5 shows that protons of this energy and greater are in the fast-background category and are discriminated against by time of flight.

The success of the over-all method in discriminating against background can be seen from the fact that a CD_2-to-C ratio of about 7:1 was obtained at most angles without using unreasonably low beam intensities.

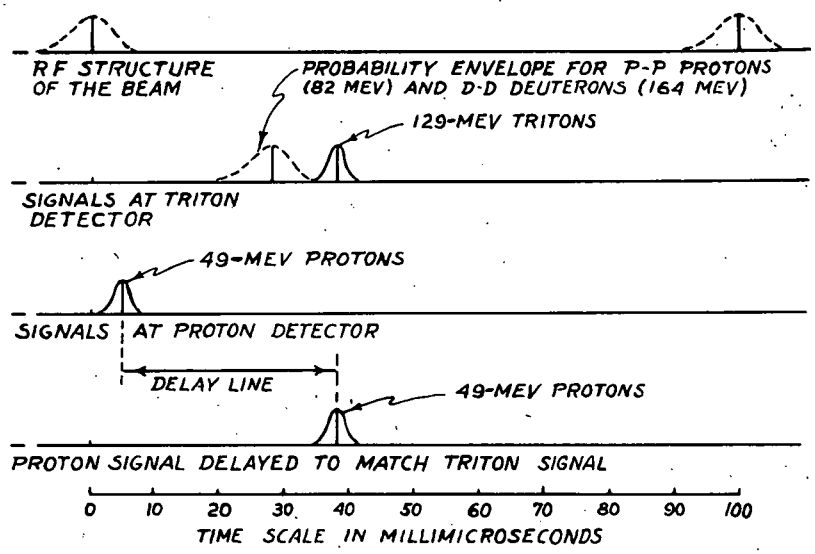

Fig. 5—Time sequence of particles arriving at the detectors. The time origin is taken as the arrival of a single radiofrequency deuteron pulse at the target.

Comparison of H^3 and He^3 Production

Beam

The experimental arrangement for comparison of H^3 and He^3 is shown schematically in Fig. 6 and a photograph of the cave with this apparatus in place is shown in Fig. 7. The incident deuterons were collimated to a beam 1 inch in diameter and monitored with an ionization chamber as previously described.

Target

In order to keep background counts at a minimum, a liquid-deuterium target was used. This system will be described in a separate paper by its designer, Mr. Roscoe Byrnes. Essentially it consists of a heat-exchange condenser. Liquid hydrogen is allowed to evaporate through a copper coil in thermal contact with another coil containing deuterium gas. Since the boiling point of deuterium is nearly 3.5°Kelvin higher than that of hydrogen at one atmosphere pressure, the deuterium is condensed and collects as a liquid in the target.

The actual target used had a volume of deuterium 1-1/2 inches in diameter and approximately 1/2 inch thick. The windows were 2-mil stainless steel. In a reservoir feeding the target were two level-sensing indicators to show when the target was empty or full. These consisted of cylindrical condensers having a capacity approximately 10 micromicrofarads for an air gap. When the gap was filled with liquid deuterium, the capacitance increased by about .3 μμf. This change was readily measured by a standard Q-meter. Blank runs were obtained by closing off one side of the deuterium target. The evaporation from the surface of the liquid built up enough pressure to force the liquid deuterium up out of the target into a reservoir. This operation required only about two minutes to perform. The blank runs, therefore, were not truly blank, since deuterium gas at approximately 21°K remains in the target. Since this experiment was a comparison of two cross sections, no error was introduced by this residual gas.

An analysis of the deuterium by Dr. Amos Newton, using a mass-spectrograph method, disclosed a composition of : 98.6% D_2, 0.54% HD, 0.84% He, and no detectable quantities of N_2, O_2 or CO_2. Since the He does not condense at liquid-hydrogen temperature, it does not contaminate

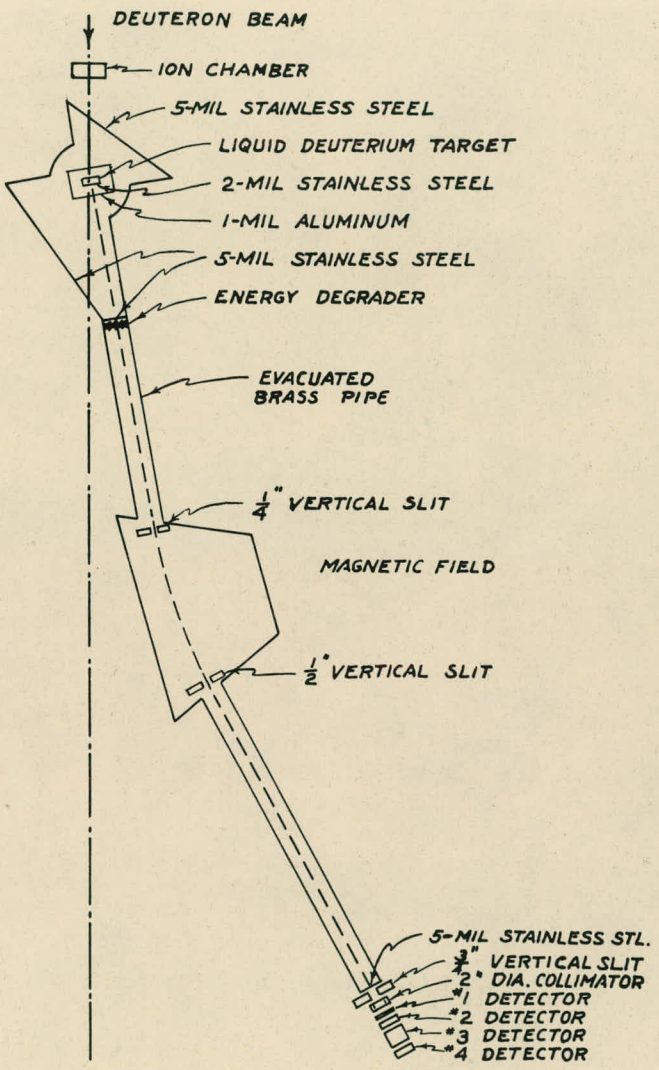

Fig. 6—Schematic diagram showing experimental arrangement for comparing production of H^3 and He^3 in deuteron-deuteron collisions.

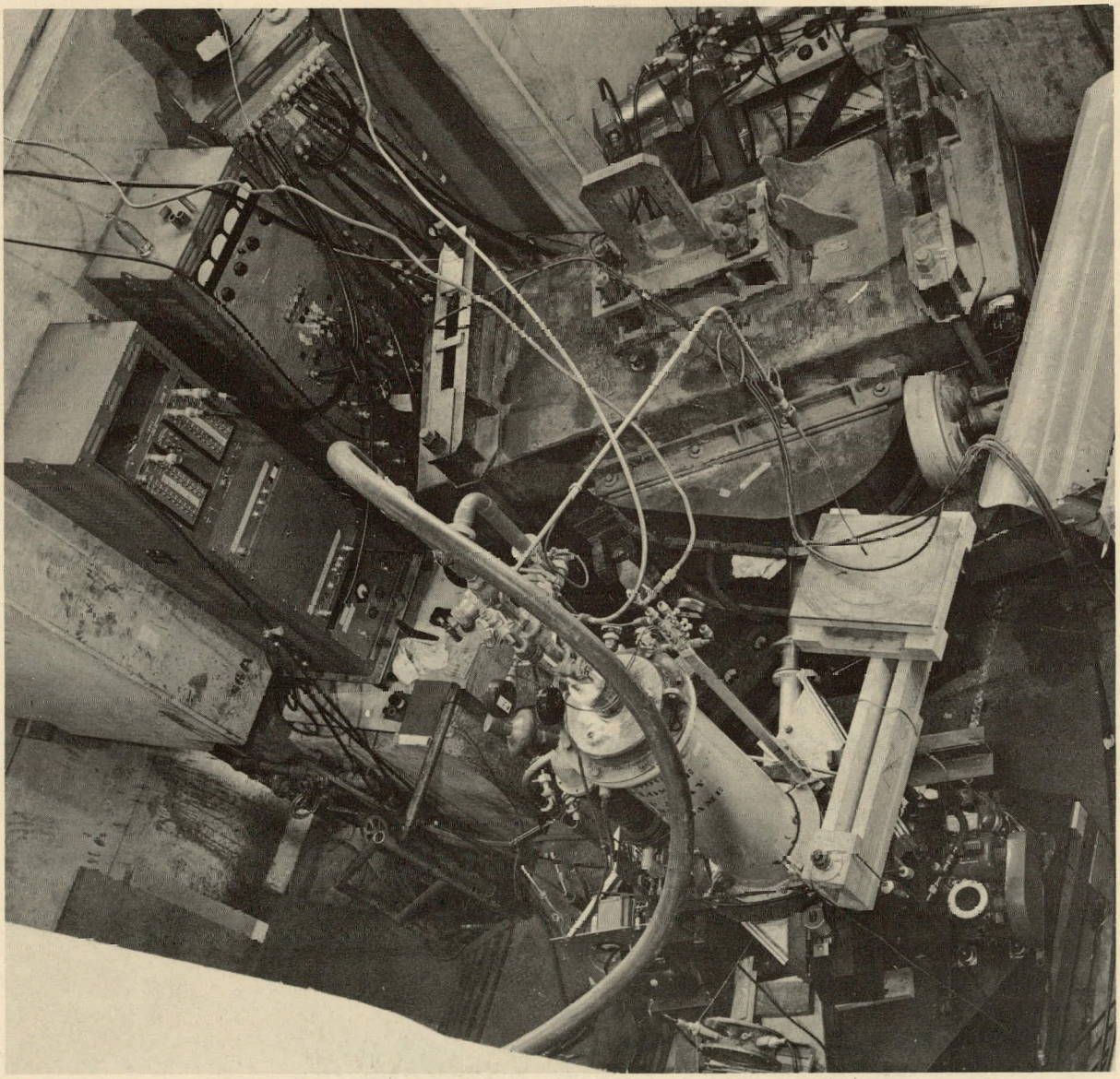

Fig. 7 — Photograph of experimental arrangement for comparing production of H^3 and He^3 in deuteron-deuteron collisions.

the liquid phase. The hydrogen cannot contribute H^3 and He^3 of the proper energy and angle.

The target was surrounded by a heat shield at liquid-nitrogen temperature. In the fore-and-aft direction this had a thickness of 1-mil aluminum. The beam entered and left the target vacuum chamber through 5-mil stainless steel windows.

Magnet

The magnet used was a pair-spectrometer magnet readily capable, with a 3-1/2-inch gap, of providing 14 kilogauss over a path length of 30 inches. The magnetic field current was set at the proper value by using wire orbit techniques (described later). This field current was determined by reading a potentiometer across a standard shunt wired in series with the field current. The potentiometer reading was checked periodically during a run. Whenever the magnetic field was increased, the field was taken to saturation and then down to the proper value. This precaution ensured that one was always on the same hysteresis curve.

Path of Particles

The H^3 and He^3 particles traversed the following path after their creation in the target (see Fig. 6): (a) a thickness of liquid deuterium ranging from 0 to 1/2 in., (b) a 2-mil stainless steel window, (c) a 1-mil aluminum window, (d) a 5-mil stainless steel window, (e) an energy degrader (for the H^3 only), which is described later, (f) a vertical slit 1/4 in. wide and 1-1/2 in. high made with aluminum blocks 1 in. thick, (g) a magnetic field of approximately 14 kilogauss for the H^3 and approximately 7 kilogauss for the He^3, (h) a 1/2-in. vertical slit made with aluminum blocks 1 in. thick, (i) a 5-mil stainless steel window, (j) a 3/4-in. vertical slit made with lead bricks, (k) a 2-in.-diameter hole in a 3/4-in. brass plate, (l) the detectors. The entire path was confined in 4-inch-diameter brass pipes which were evacuated to a pressure of at most 100 microns.

The location of these various elements was determined by using the well-known current-carrying wire to trace the orbit of the particle. The method is based on the formula

$$P = K \frac{F}{I}$$

where P is the relativistic momentum of the charged particle whose orbit is to be determined, K is a constant whose numerical value depends upon the units and the charge on the particles, F is the tension in the wire, I is the current in the wire. If the above formula is fulfilled, the orbit taken up by the wire in any magnetic field corresponds to a trajectory of the particle. Since the momentum (P) of the H^3 and He^3 for any given scattering angle is determined, one has only to pick any arbitrary tension (F) and calculate the required current (I) from the above formula.

The procedure used was as follows: A wire was strung down the channel from the center of the target to the center of the detector. Tension was provided by a 500-gram weight strung over a pulley. The calculated current (I) for a H^3 of proper energy was applied through the wire. The magnetic field was adjusted so that the wire passed down the centers of the brass pipes. The collimating slits were all put in position so that the wire bisected them. The magnetic-field potentiometer reading was recorded. Next the calculated current (I) for a He^3 of proper energy was applied to the wire. The magnetic field was then adjusted so that the wire again bisected the channel and collimating slits. The magnetic-field potentiometer reading was recorded. Thus a single physical channel was defined, which could be adjusted to accept either H^3 or He^3 of the proper energy by changing the magnetic field. The possible products of a deuteron-deuteron collision that would be accepted by the channel are listed in Table I.

TABLE I

Desired Particle	Mean Energy of Deuteron-Deuteron Collision Products With Same Hρ (Mev)			
	Protons	Deuterons	H^3	He^3
H^3	400	230	159	600
He^3	115	60	40	159

The energy degrader is shown in Fig. 8. It was placed in position as shown in Fig. 6 for H^3 and removed for He^3. It had a dual function: one to provide the same spread in energy of the H^3 as for the He^3, the other to provide the same multiple scattering for both H^3 and He^3. It was essential that the energy distributions of the two particles be identical, unless one could guarantee detecting all particles which passed through the first collimating slit. Even if the particles passing through the first slit were perfectly collimated, they would be spread out horizontally across the face of the detector if they were not monoenergetic. If this distribution function were wider than the detectors, then the number of particles going through the detector would depend upon the energy spread. Since He^3 had an energy of 163 ± 6 Mev after leaving the target, the actual horizontal distribution function at the detectors was determined much more by the finite size of the target and collimating slits than by the energy spread. Even without the degrader, therefore, the errors due to the different energy spreads would have been small.

The principle of the degrader is obvious from Fig. 8. Particles go through different thicknesses of absorber and suffer various energy losses. Ideally, if the grooves were very close together, the energy losses would be quite random horizontally. Since the horizontal distance across the degrader to go from maximum attenuation to minimum attenuation is only 1/16 inch, it was felt that the random ideal was approached. The depth of the grooves was calculated to equalize the H^3 energy spread to that of the He^3. The residual thickness of the degrader was calculated to equalize the multiple scattering of the mean H^3 to that of the He^3. Fortuitously this also served to drop the mean energy of the H^3 to a value equal to that of He^3.

The exact value of the magnetic field was later checked during the run by varying the magnetic field of the magnet over a range of values close to the calibrated value, and plotting the counting rate. A magnetic field was used corresponding to the peak of the counting rate. The value of the field thus determined was found to lie very close to the expected value.

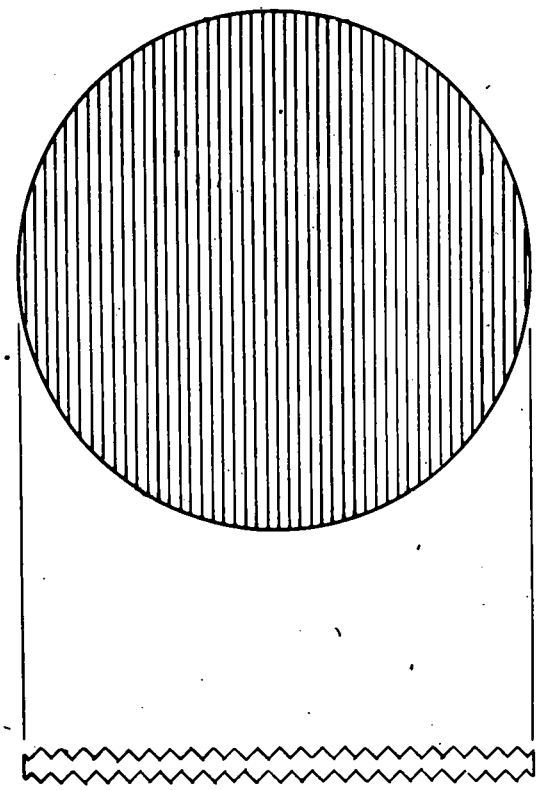

Fig. 8—Energy degrader for H^3.

Detectors

A schematic representation of a typical detector is shown in Fig. 9. A liquid cell 2-7/8 inches in diameter was viewed by three photomultiplier tubes. The pulses of two 1P21 tubes were added and used to drive a coincidence circuit. A single 5819 was connected to the cell by a lucite light pipe. These pipes were of the adiabatic taper type discussed by Garwin,[19] except for the largest counter, whose area in the direction of viewing was much larger than the 5819 photocathode area. In this case the pipe tapered in toward the photocathode in both dimensions. The coupling between the 5819 and the light pipe was made with a commercial hard-setting transparent plastic. A mirror was used on the side of the cell opposite the 5819 to provide a more symmetrical light distribution. The liquid phosphor employed was one developed by Kallman:[20] 0.3 percent p-terphenyl and 0.001% diphenylhexatriene (by weight) dissolved in phenylcyclohexane. All photomultiplier tubes were magnetically shielded.

Three pulse-height detectors were employed whose thicknesses were 0.2 inches, 0.6 inches and 2.4 inches. The first detector served to measure dE/dx of the He^3. The second detector served to measure both E of the He^3 and dE/dx of the H^3. The third detector served to measure the E of the H^3. The fourth detector was merely a liquid cell viewed by one 1P21 tube. Since the desired particles did not have sufficient energy to get into this detector, any particle making a pulse in this detector could be discarded. The energy losses calculated for the four detectors are listed in Table II. Calculations were based on Aron's data.[21]

TABLE II

Energy Loss (Mev)

Particle	Initial Energy (Mev)	1st Detector	2nd Detector	3rd Detector	4th Detector
H^3	159	5	16	126	-
He^3	159	23	114	-	-

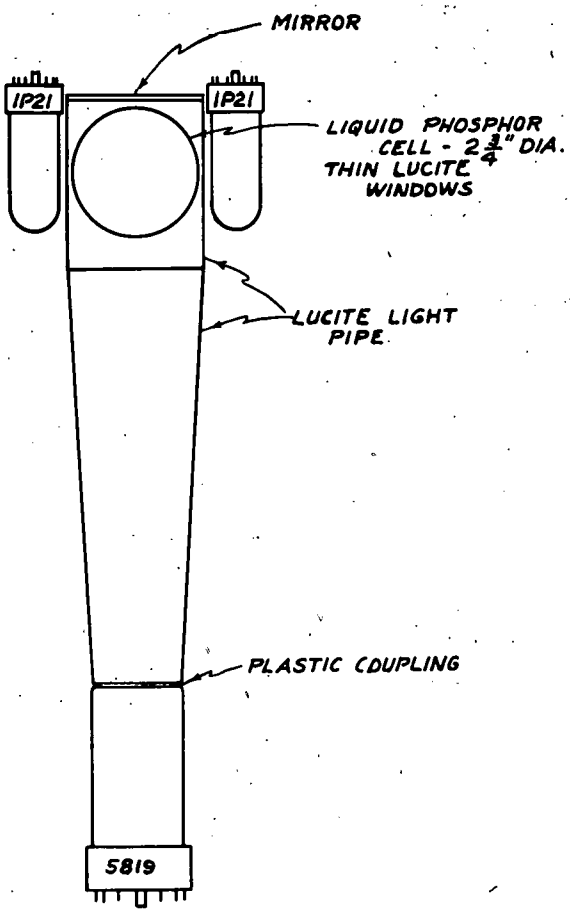

Fig. 9—Schematic diagram of typical pulse-height detector.

A 2-inch brass collimator was used just ahead of the second detector. (See Fig. 6) This collimator served to define the sensitive counting area, and its size was picked so that the probability of a particle's scattering out of the final counter would be negligible. The calculations on scattering were based on data of Millburn and Schecter.[22]

Electronics

A block diagram of the electronics is shown in Fig. 10. Double coincidences were made either between the first and second detector (for He^3) or between the second and third detector (for H^3). The pulse-shaping and coincidence units were similar to those previously described. Amplified outputs from the coincidence unit were used to trigger the sweep of the oscilloscope and to drive a scaler. The use of separate photomultipliers to provide coincidence pulses and pulse-height pulses was considered advantageous, so that optimum voltages could be used on each and so that a fast coincidence could be made. As previously noted, the resolving time of the coincidence unit was about three millimicroseconds. The success of this circuit in eliminating accidentals can be seen from the fact that plugging the magnetic channel when running at full beam intensity reduced the coincidence counts essentially to zero.

The pulse-height signals themselves were delayed with respect to each other in order to separate them on the oscilloscope screen, were added in a resistive adder, and then fed into a Tektronix model 517 oscilloscope. A regulated power supply was used to furnish power to all components of the circuit.

Photographic Apparatus

The oscilloscope face was coupled to a General Radio 35-mm oscilloscope camera by a hood furnished with a peephole. The film was moved continuously at a very slow rate of speed, since the counting rate was only of the order of 5 to 10 counts per minute. The film used was Eastman Linagraph Pan. With a sweep speed of 50 millimicroseconds per cm. and an aperture of f/1.5, the oscilloscope intensity could be used at well below its maximum setting to give a very fine line. Several sample traces are shown in Fig. 18. Sample strips were developed periodically during a run to check the performance of the equipment.

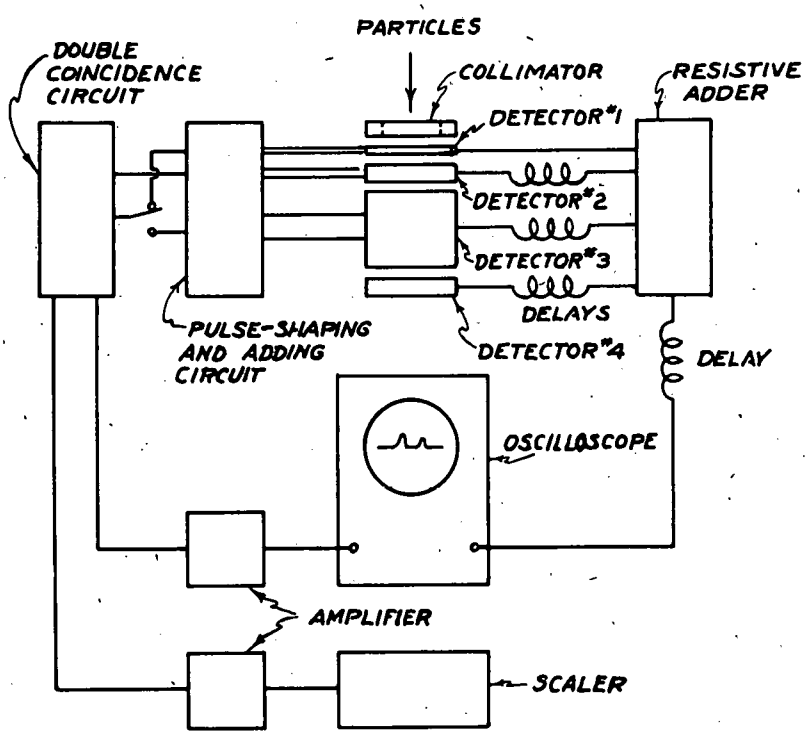

Fig. 10—Block diagram of electronics for comparing H^3 and He^3.

Experimental Procedure

The first step in conducting a run was to line the target up in the beam. This was done with the help of X-ray film exposed behind the target.

The next step was to calibrate the detectors. The detector telescope was placed directly in the deuteron beam. The beam itself was reduced to several counts per second. By means of absorber placed in front of the detectors, it was possible to get monoenergetic deuterons of known energy. Using Aron's data[21] to calculate the energy losses of these deuterons and the desired H^3 in the detectors, it was possible to set the voltages of the 5819 photomultipliers at a level that would give about 1 cm. deflection on the oscilloscope for H^3. The oscilloscope amplifier became nonlinear at deflections over 1 centimeter. The 1P21 photomultiplier voltage settings for H^3 coincidences and He^3 coincidences were then determined by using deuterons whose energy losses most closely simulated those of the desired particles. The pulses from the E detector were made roughly equal to those of the dE/dx detector by actually looking at the inputs to the coincidence unit. Since the deuterons used had energy losses less than those expected of the desired particles, and since the oscilloscope trigger was set at a considerably lower bias than was necessary to detect these deuterons, 100 percent efficiency for detecting the H^3 and He^3 was insured. In this experiment, a counting plateau is not necessary or desirable. The bias can be set low and the pulse-height analysis can discard the low-energy pulses.

Next the detector telescope was placed back in position at the far end of the channel. The coincidence inputs and the magnetic field were set for He^3. The target was filled with liquid deuterium. Since the He^3 particles were readily distinguishable from other particles on the oscilloscope screen, it was possible to adjust the 5819 voltages to give approximately 1 cm. deflection for both the dE/dx and E detectors. The magnetic field was then changed slightly to maximize the counting rate as outlined previously. The camera was turned on and allowed to record the pulses for a certain number of integrated volts on the beam monitor. A similar record was made with a blank target.

To switch to H^3, the inputs to the coincidence unit were changed from the first and second detectors to the second and third detectors. The

energy degrader was put in place and the magnetic field set for H^3. The magnetic field was then adjusted to maximize the counting rate. It was not possible to distinguish the H^3 visually on the oscilloscope screen, and it was necessary to use the scaler counts to determine the peak. Since the majority of the scaler counts were H^3, the peak was determined with sufficient accuracy. The camera was again turned on and allowed to record pulses, using first a liquid-deuterium and then a blank target.

Finally, without changing the voltages or relative positions of the detectors, the detector telescope was placed back in the beam and a photographic record was taken of pulses from deuterons ranging from 110 Mev up to 155 Mev, obtained by placing various absorbers in front of the detectors. These data later served to give the resolution of the detectors and to provide a calibration for deuterons that might have to be distinguished from H^3.

RESULTS OF THE EXPERIMENT

Differential Cross Section for $d + d \rightarrow H^3 + p$

Identification Data

The first step in identifying the process was to make sure there were no accidental counts, and to make sure the process being observed came from deuteron-deuteron collisions. If so, the net counting rate should not change with variations in beam intensity. The result of varying the deuteron-beam intensity for one scattering angle is given in Table III.

TABLE III

Relative Beam Intensity	CD_2 - C Difference Rate	CD_2 to C Ratio
5	10.4 ± 0.9	3.5 : 1
1	10.5 ± 1.1	11.5 : 1

Although the background counting rate from carbon went up with increasing beam intensity, the net counting rate remained the same.

To show that the deuteron-deuteron process being observed was actually that postulated, the angles, time-of-flight delay, and absorbers were next changed. This identification was made at the scattering angle of 45° center-of-mass.

The angular correlation was tested by moving the triton detectors horizontally away from the calculated position. The results, plotted in Fig. 11, show that the difference rate essentially disappeared in moving approximately twice the width of the detectors. The coplanarity of the process was tested by raising the triton detectors. The results, plotted in Fig. 11, show that the difference rate disappeared in moving twice the height of the detectors.

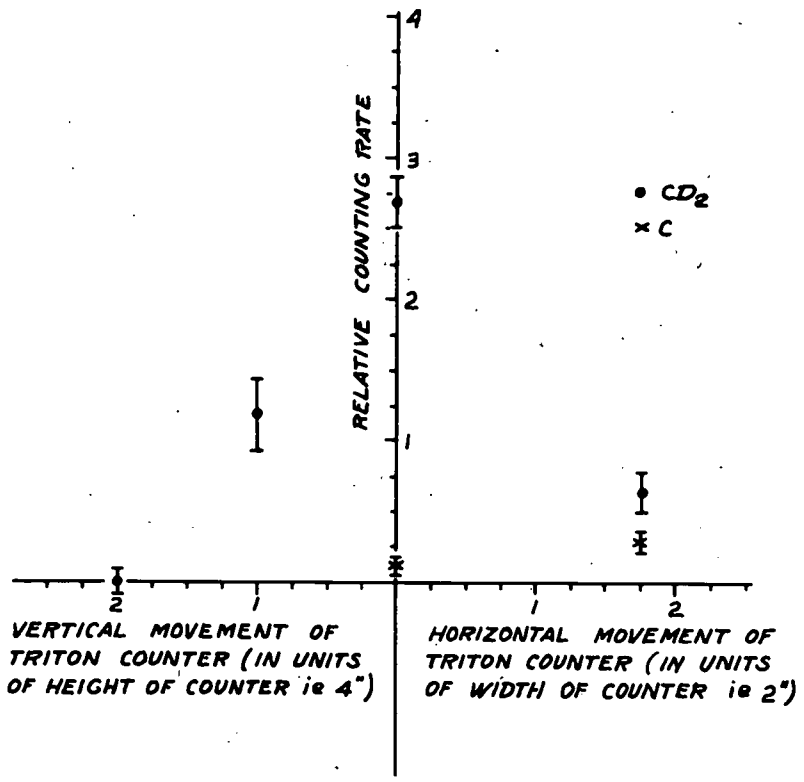

Fig. 11—Angular and coplanar correlation test for the process $d + d \rightarrow H^3 + p$.

The time-of-flight correlation was tested by changing the delay of the proton signal into the coincidence circuit. The results are plotted in Fig. 12. The difference rate disappeared on increasing or decreasing the proper delay by approximately twice the resolving time of the coincidence unit. As the delay was decreased, however, the carbon background began to increase. This illustrates how effective the time of flight was in discriminating against this background.

Next the absorbers were changed to test the range correlation. The absorbers in front of the detectors were increased to that amount necessary to just stop the most energetic postulated particle before entering the last detector. The results are plotted for the triton and proton detectors, respectively, in Figs. 13 and 14. In both cases the net counting rate disappeared. Figure 13 shows also the effect of removing the absorbers in front of the triton detectors. Although the carbon background increased, the net counting rate remained the same.

The above tests were considered adequate evidence that the process being observed was indeed the $d + d \rightarrow H^3 + p$.

Angular Distribution Data

Data for an angular distribution were taken at six laboratory angles chosen to cover as nearly as possible the center-of-mass scattering range of 0° to 90°. These uncorrected data are summarized in Table IV.

TABLE IV

Triton CoM Angle	Difference of CD_2 and C Rates	Ratio of CD_2 to C Rates
20°	7.69 ± 0.85	2.3 : 1
30	6.88 ± 0.76	5.3 : 1
45	10.31 ± 0.65	7.4 : 1
60	5.23 ± 0.36	5.3 : 1
75	24.7 ± 2.9	7.5 : 1
85	10.9 ± 1.0	12.0 : 1

This difference rate is the counting rate, R, that appears in the cross-section formula on page 38.

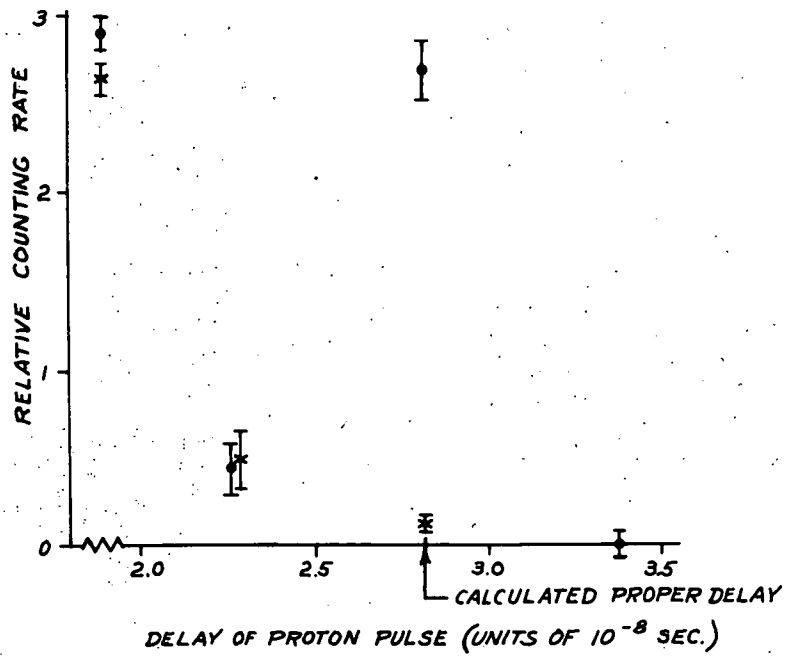

Fig. 12 — Time-of-flight correlation test for the process $d + d \rightarrow H^3 + p$.

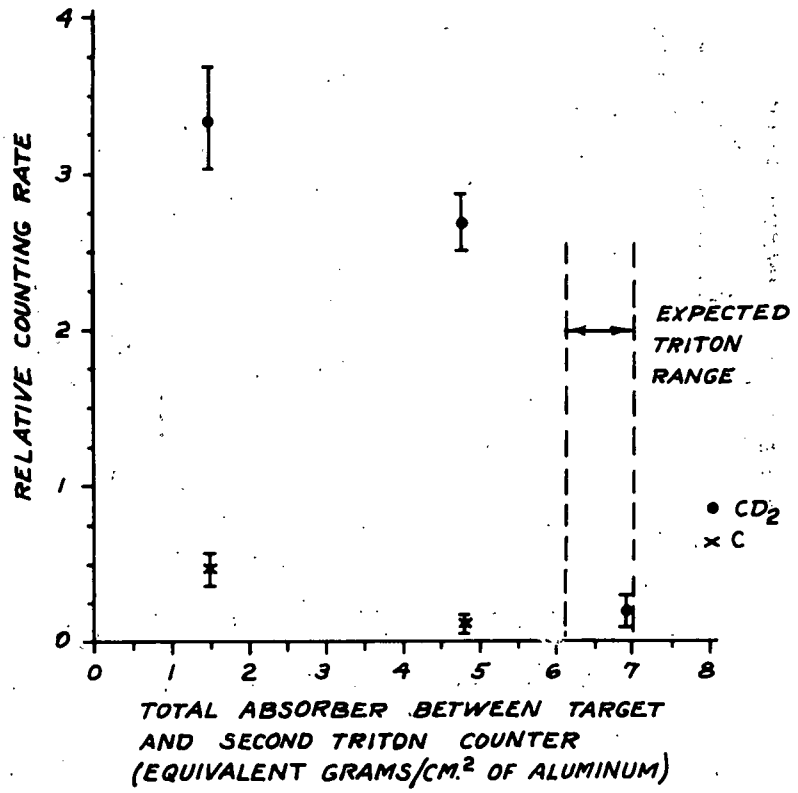

Fig. 13—Range correlation test of particles arriving at H^3 detector.

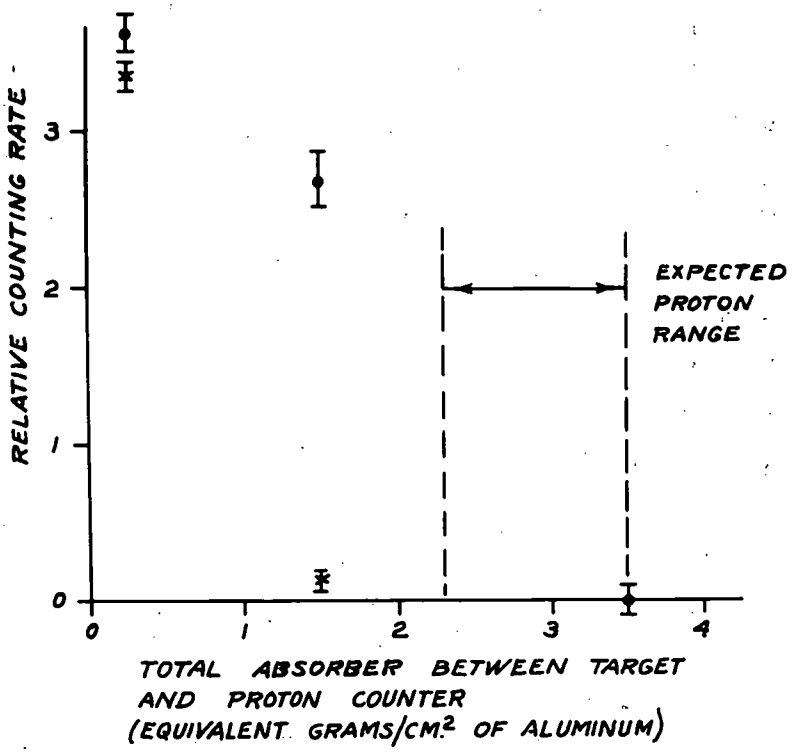

Fig. 14—Range correlation test of particles arriving at proton detector.

The apparent high counting rates for the last two readings are due to the use of a monitor for these data with a calibration differing by a factor of ten from that used for the other data.

Three corrections were applied to the original difference-counting rate. The first was for absorption of protons in passing through the aluminum absorber. This correction was calculated from the absorption cross sections measured by Kirschbaum.[23] The correction was only seven percent in the worst case.

The second correction was for absorption of the tritons in the aluminum absorbers or in the first stilbene crystal. It is not possible to make a rigorous correction for this effect. The following attack was employed to give an estimate of the correction: W. Crandall[24] has measured the total inelastic cross section of high-energy He^3 particles for various elements. Assuming that the probability of a nuclear event at high energy is the same for a H^3 as for a He^3, it is possible to calculate the attenuation of the tritons in going through the absorber. The majority of the inelastic events, however, constitute stripping processes in which, approximately two-thirds of the time, a fast deuteron continues in the forward direction. Since these deuterons, in general, still produce pulses in the triton detector, only about one-third of the inelastic events are lost. Since the inelastic attenuation in the worst case was 21 percent, the maximum correction is around 7 percent.

The third correction was that for small-angle scattering losses. These losses were minimized by having the proton detector subtend a considerably larger solid angle than the triton detector. Under these conditions, the worst correction amounted to 8 percent. The method of calculation is outlined in the Appendix.

The correction factors are summarized in Table V.

TABLE V

Triton CoM Angle	Proton Absorption	Triton Absorption	Scattering	Total
20°	1.00	1.07	1.07	1.14
30	1.00	1.06	1.03	1.09
45	1.00	1.05	1.08	1.13
60	1.01	1.03	1.07	1.11
75	1.04	1.02	1.08	1.15
85	1.07	1.01	1.08	1.17

The center-of-mass differential cross section is obtained from the relation

$$\frac{d\sigma}{d\Omega_o} = \frac{R \quad C}{N_b \, N_t' \, \Delta\Omega_o}$$

The numerator is the product of the original difference rate, R, and the total correction factor, C. N_b is the deuteron beam flux in deuterons per integrated beam unit; it is calculated from the ion-chamber calibration factor and the capacitance of the integrating condenser. N_t is the target particle density in deuterons per square centimeter; it depends on the weight, area and composition of the target and the angle made by the target with respect to the beam. The term $\Delta\Omega_o$ is the center-of-mass solid angle subtended by the triton detector; it is calculated from the laboratory solid angle by means of the calculated relativistic transformation. The final results are given in Table VI and plotted in Fig. 15. Figure 16 shows the same data on a semi-log plot.

TABLE VI

Triton CoM Angle	$\frac{d\sigma}{d\Omega_o}$ (Millibarns/steradian)
20^o	1.54 ± 0.17
30	0.905 ± 0.100
45	0.258 ± 0.016
60	0.0871 ± 0.0060
75	0.0486 ± 0.0057
85	0.0317 ± 0.0029

It is interesting to note that the cross section seems to fall off exponentially for scattering angles up to 60^o. This behavior is referred to later.

The errors shown are the statistical deviations related to the number of counts constituting the original data. The errors in N_b, N_t and $\Delta\Omega_o$ have been neglected as far as relative angular-distribution data are concerned, since they are the same for each angle and affect only the total absolute cross-section. The error in N_b is estimated to

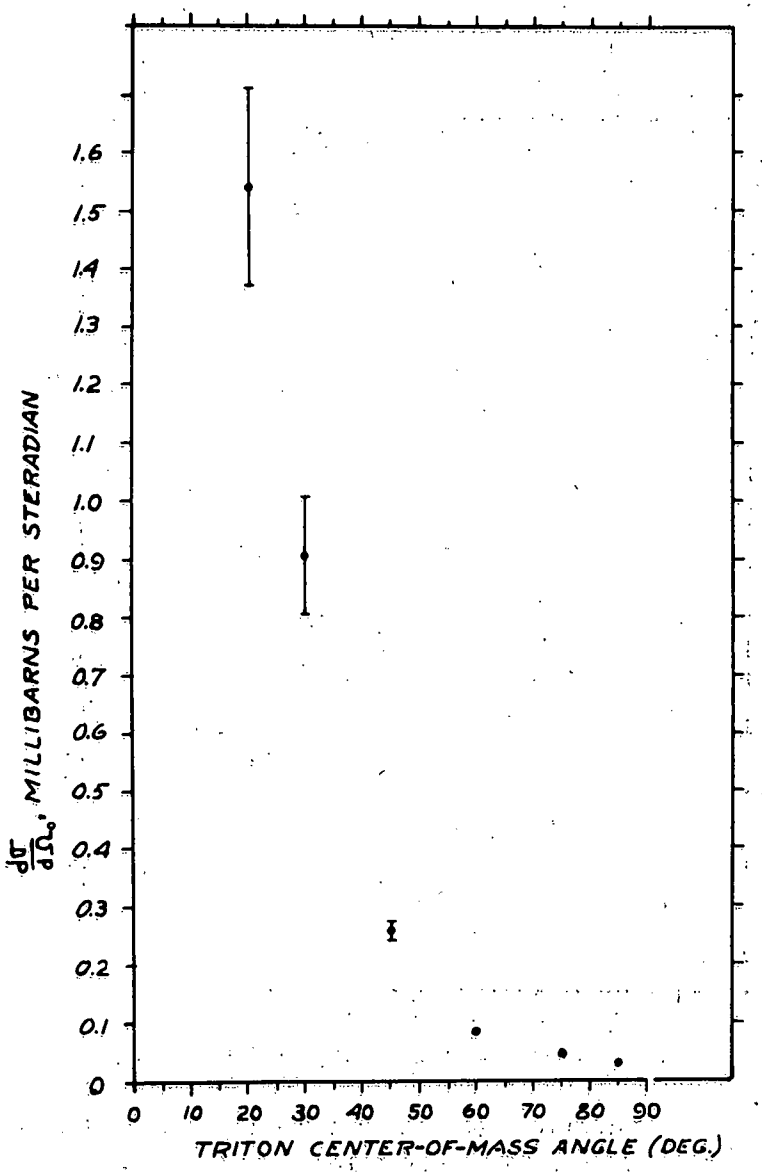

Fig. 15 — Experimental angular distribution for the process $d + d \rightarrow H^3 + p$ on Cartesian coordinates.

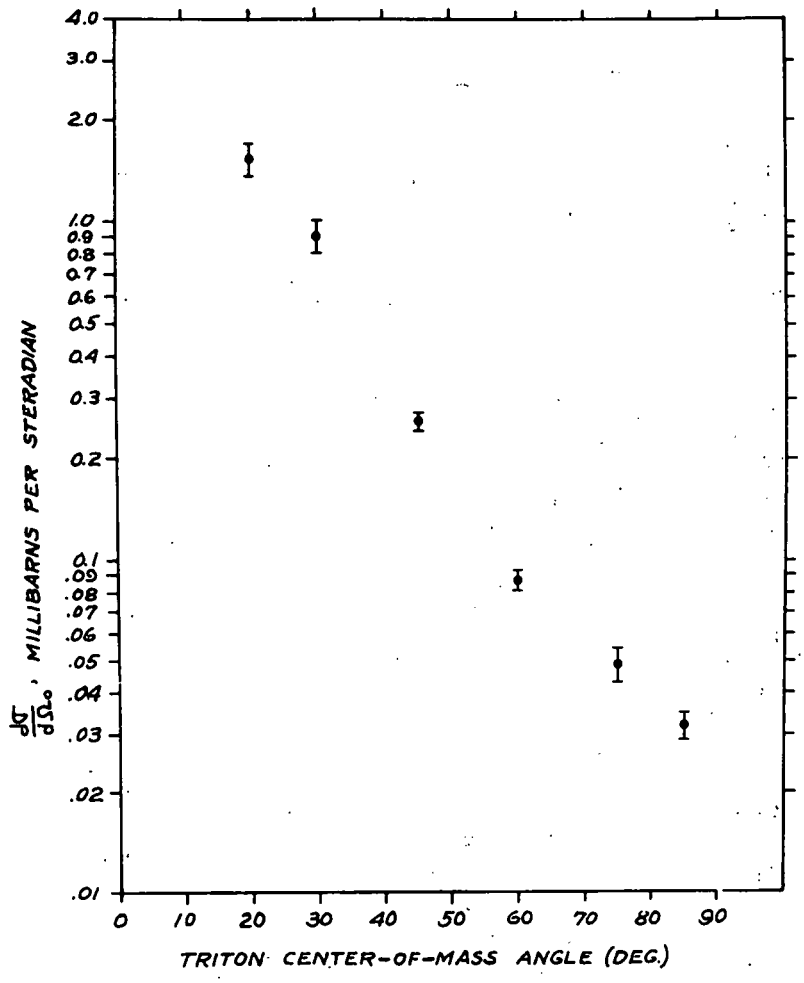

Fig. 16—Experimental angular distribution for the process $d + d \rightarrow H^3 + p$ on semi-log coordinates.

be several percent; in N_t about 1 or 2 percent; and in $\Delta \Omega_o$ around 5 percent. The corrections to the data are relatively small, but if it is assumed that they could contribute an error of 5 percent, one can estimate that the absolute results have an uncertainty of about 15 percent. By drawing a smooth curve through the data of Fig. 16 one estimates the integrated total cross section to be 4.1 millibarns.

Conclusions

An understanding of the mechanism for the production of tritons in the reaction $d + d \rightarrow He^3 + p$ can be facilitated by invoking the law of detailed balance and considering instead the inverse process $p+H^3 \rightarrow d+d$. One now postulates that there is a sudden interaction between the proton and one of the H^3 nuclei, and further that the momenta of the other two H^3 nuclei are essentially unaffected by the interaction. Two cases are of interest: one where the two interacting nuclei end up in the same deuteron, the other where they end up in different deuterons. Momentum diagrams for these two interactions are shown in Fig. 17. Both these processes have been observed in the proton bombardment of nuclei. The first situation is identical to the pickup mechanism proposed by Chew and Goldberger[25] to explain the presence of fast deuterons in the forward direction when matter is bombarded with high-energy protons or neutrons. The second situation might be called an indirect pickup, since it consists of a proton's scattering in a nucleus and then finding a pickup partner of momentum consistent with the formation of a deuteron. This indirect pickup process could contribute to the scattering process at wide angles where the pure pickup cross section would be negligible. W. Hess is measuring the indirect pickup cross section for various elements using 360-Mev protons. Preliminary results[26] indicate that most of the deuterons observed at 40^o laboratory system for p - d scattering are a result of indirect pickup rather than pure pickup.

In the $p + H^3 \rightarrow d + d$ process, one would expect a comparatively low cross section, since the momenta must be favorable to the formation of two deuterons instead of just one. In the pure pickup interaction, for example, not only must the two interacting particles form a deuteron, but also the two remaining H^3 nuclei must be left in a state corresponding to that of a deuteron.

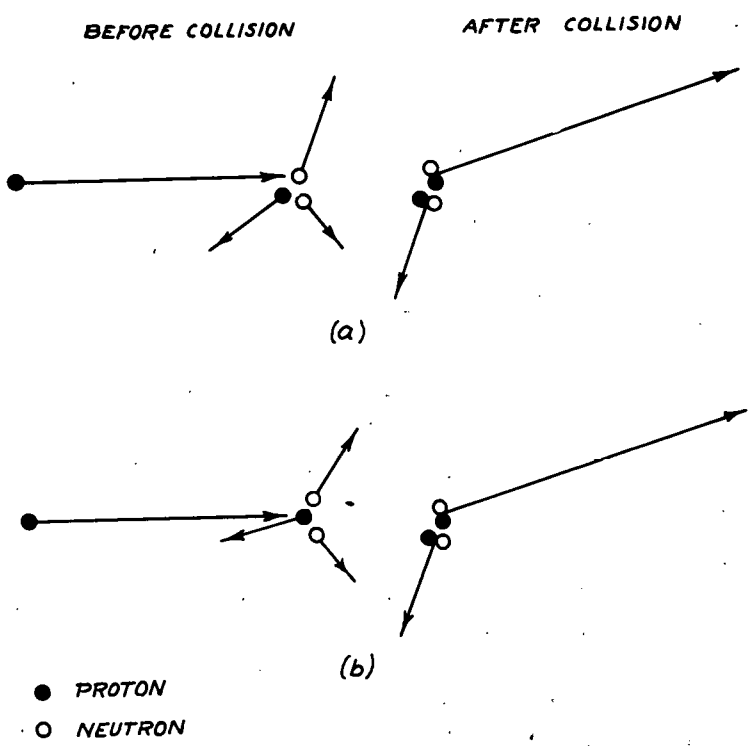

Fig. 17—Diagram showing typical laboratory momenta of particles before and after collision in the $p + H^3 \rightarrow d + d$ process: (a) for pure pickup interaction, (b) for indirect pickup interaction resulting in same external momenta.

Using the Born approximation, Drs. Bludman and Heckrotte set up the integrals for the matrix elements of the cross sections for the two interactions postulated above. The pure pickup cross section was readily solved in terms of the momentum distributions of the deuteron and the triton. Assuming the Hulthén wave function for the deuteron and the wave function proposed by Messiah for the triton, the distribution of the $d + d \rightarrow H^3 + p$ cross section was calculated. It was found to behave exponentially in the forward direction in a manner similar to the experimental data. The slope of the theoretical curve, however, was greater than that of the experimental curve. The theoretical cross section became negligible at wide angles.

Unfortunately, the integral for the indirect pickup interaction was too difficult to solve without an undue expenditure of time. One concludes that the pure pickup (or stripping) mechanism can explain qualitatively the shape of the cross section for scattering angles up to about 45° CoM, but that substantial contributions must be made by other processes.

Comparison of H^3 and He^3 Production

Reduction of Data

Final data were read from the developed film by projecting in a Recordak Microfilm viewer having a magnification factor of about 19. The camera reduced the pulse size by a factor of 4.4 on the 35-mm. film. Therefore, the 1-cm. pulses on the oscilloscope screen were about 4.3 cm. on the screen of the Recordak. Pulse heights were estimated to the nearest millimeter on the screen.

Typical pulses are shown in Fig. 18. The spacing between pulses was due to the delay introduced as previously described. Very little jitter was detected in either the sweep position of the pulses or the relative spacing of the pulses. Spurious pulses not correlated in time to the other pulses were very seldom seen on the traces. Accidental coincidences were detectable for the H^3 run when a pulse was seen from the second and third detector but there was nothing on the first. These counts were very infrequent and the pulses were invariably small. No record was made of the pulse height of the first detector when detecting H^3, since the second detector provided a dE/dx pulse

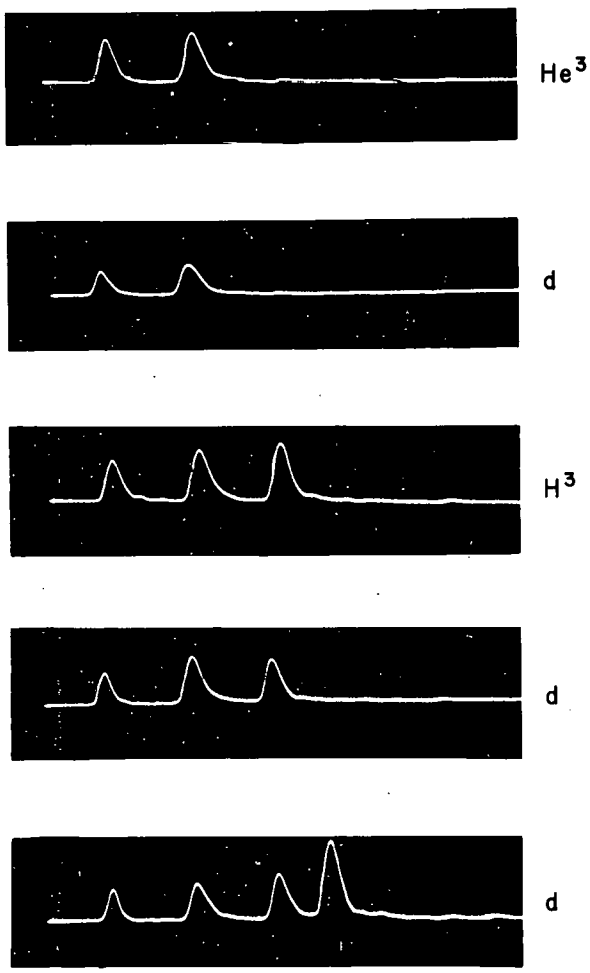

Fig. 18 — Film traces of typical He^3, and H^3 and background pulses.

with better resolution. Fast protons and deuterons that went through the first three detectors were readily identified by noting a pulse from the fourth detector. No record was kept of the height of the fourth pulse; the responsible particle was merely identified as a "pass-through" in plotting the data.

The heights of the pulses from the dE/dx and energy detectors were recorded orally on a Sound Scriber as a pair of numbers. These recordings were then played back and the data were plotted. The pair of numbers from each pattern was plotted as a point on graph paper with dE/dx pulse height as ordinate and energy pulse height as abscissa. Patterns without a pass-through were plotted as dots; those with a pass-through as crosses.

The Analysis of Data

In Figures 19 and 20 are plotted the calculated energy losses of various particles traversing the detector system. Figure 19, for example, shows that He^3's of various energies fall along a line. If the mechanism by which the energy loss of the particle is converted to pulse height were perfectly linear, these curves would also represent the pulse-height locus for He^3's of various energy (assuming the scales to be suitably chosen). Owing primarily to saturation effects in the detector for high values of specific ionization and to non-linearity of the amplification system, one would not expect the actual pulse-height locus to have the same slope or position as the energy-loss curve. The over-all resolution of the detecting system, moreover, as manifested by the Landau[27] effect, the statistical fluctuation in the number of photoelectrons released from the photocathode, and the optical resolution of the detector, spread the expected line out into a band. The width of this band is a direct measure of the over-all resolution.

In Figs. 19 and 20, therefore, the general regions outlined are where pulse-height pairs were expected to fall. The energies of the particles in these regions correspond to the energies of the particles that can come down the channel as listed in Table I.

Figure 21 shows the total data collected for He^3 with liquid-deuterium target and Fig. 22 with blank target. Figures 23 and 24 show the corresponding data for H^3. The He^3 data are unambiguous. The

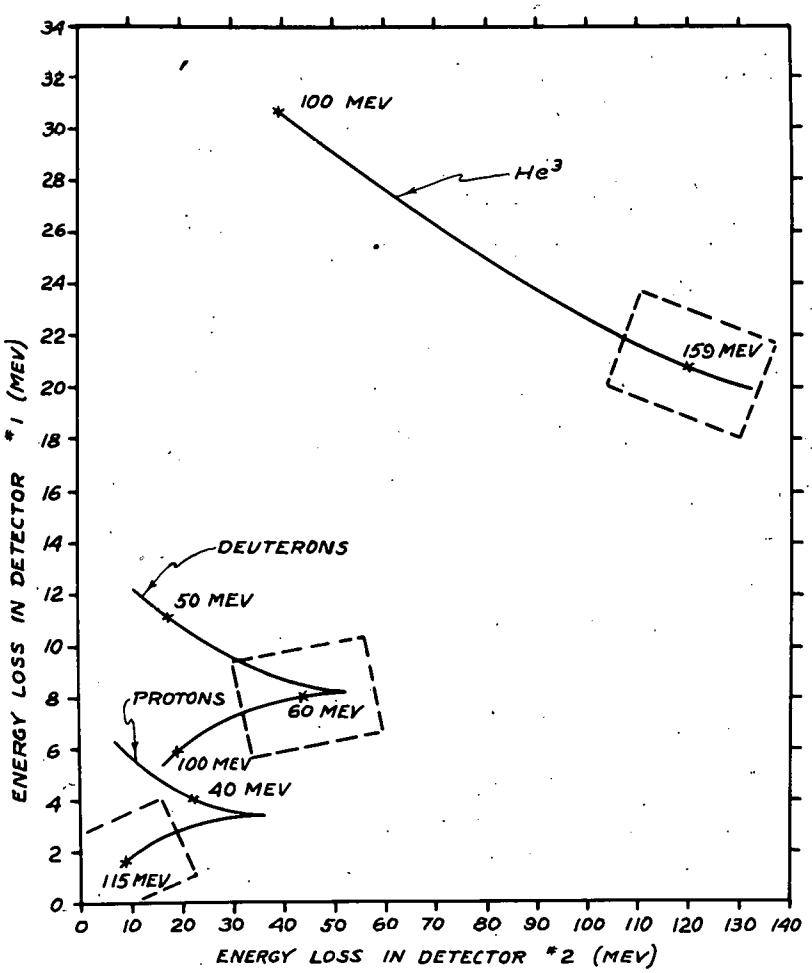

Fig. 19—Plot of calculated energy loss in first detector vs. calculated energy loss in second detector for He^3 and other particles. Areas outlined indicate regions where pulses expected to lie.

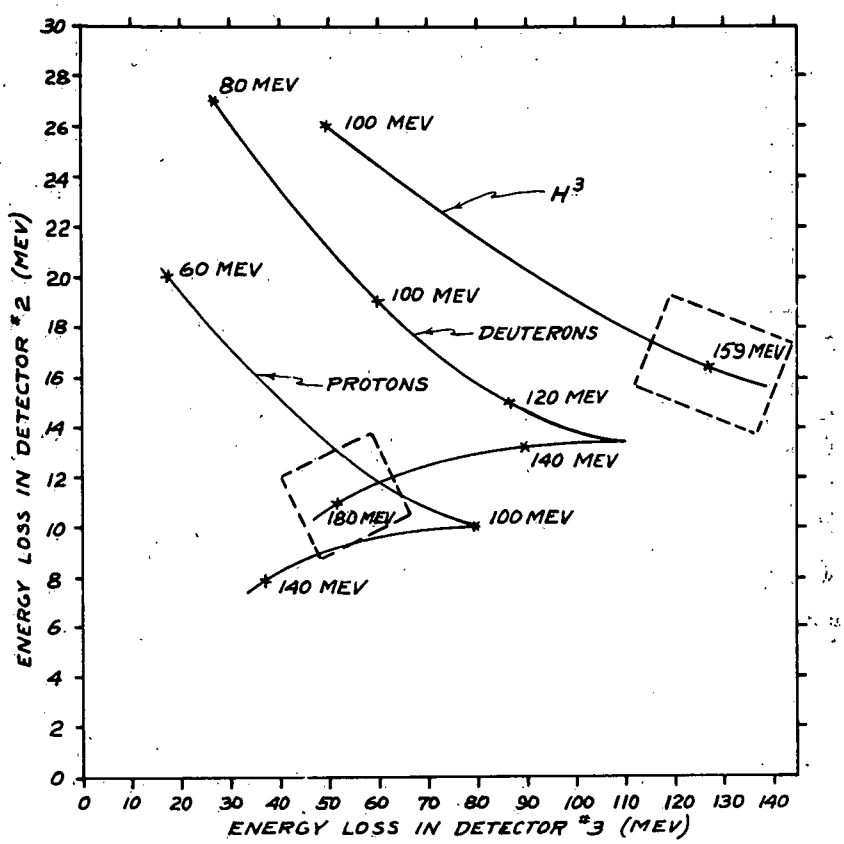

Fig. 20—Plot of calculated energy loss in second detector vs. calculated energy loss in third detector for H^3 and other particles. Areas outlined indicate regions where pulses expected to lie.

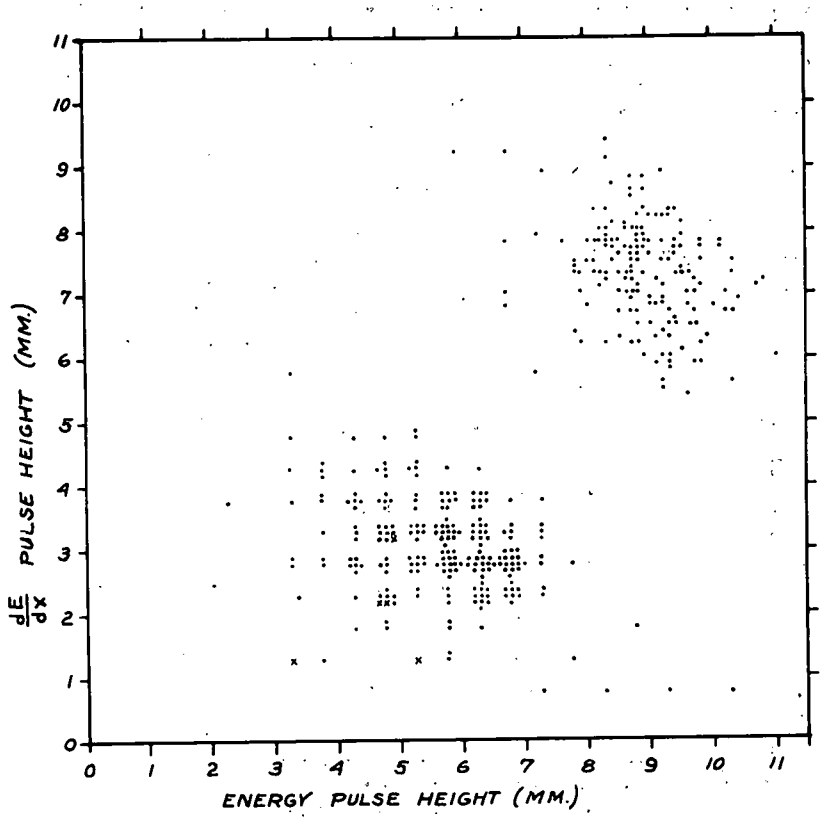

Fig. 21 — Final data for counting rate of He^3 using liquid deuterium target. Data obtained in 10 integrated beam units.

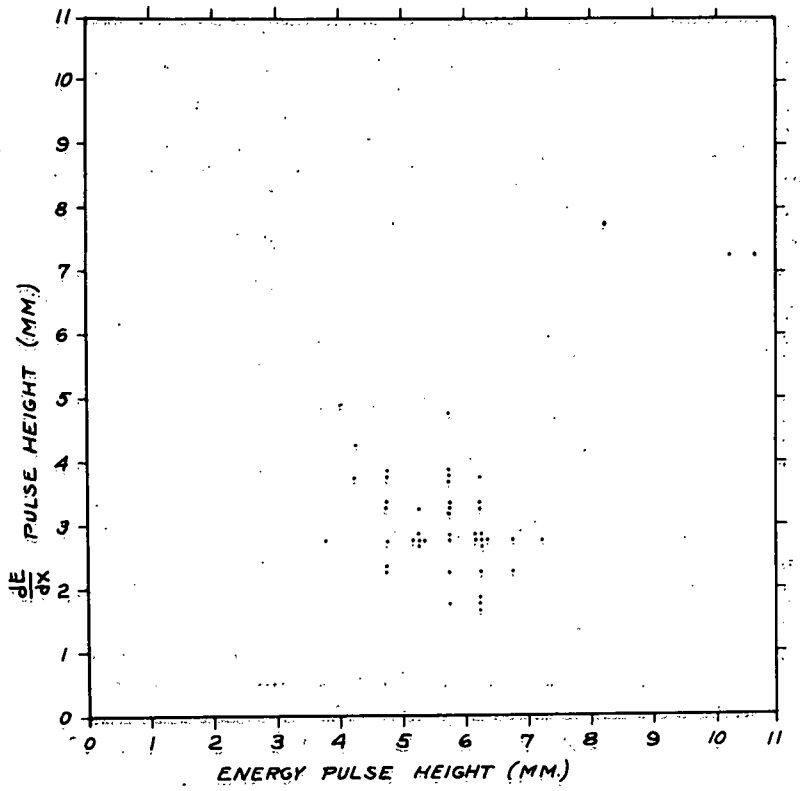

Fig. 22 — Final data for the counting rate of He^3 using blank target. Data obtained in two and one-half integrated beam units.

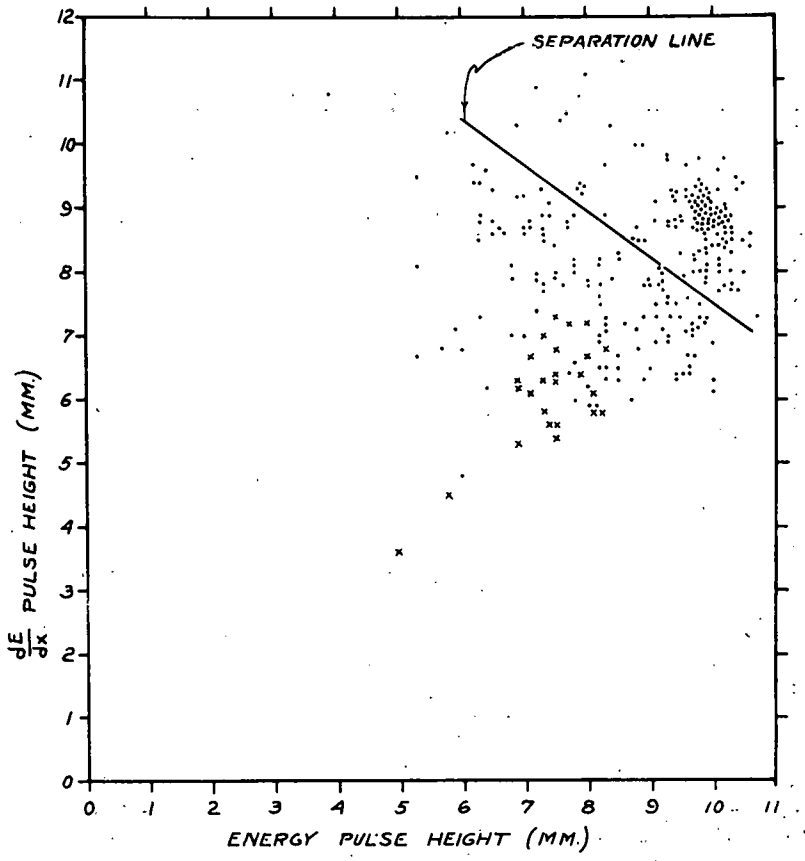

Fig. 23 — Final data for counting rate of H^3 using liquid deuterium target. Data obtained in 10 integrated beam units.

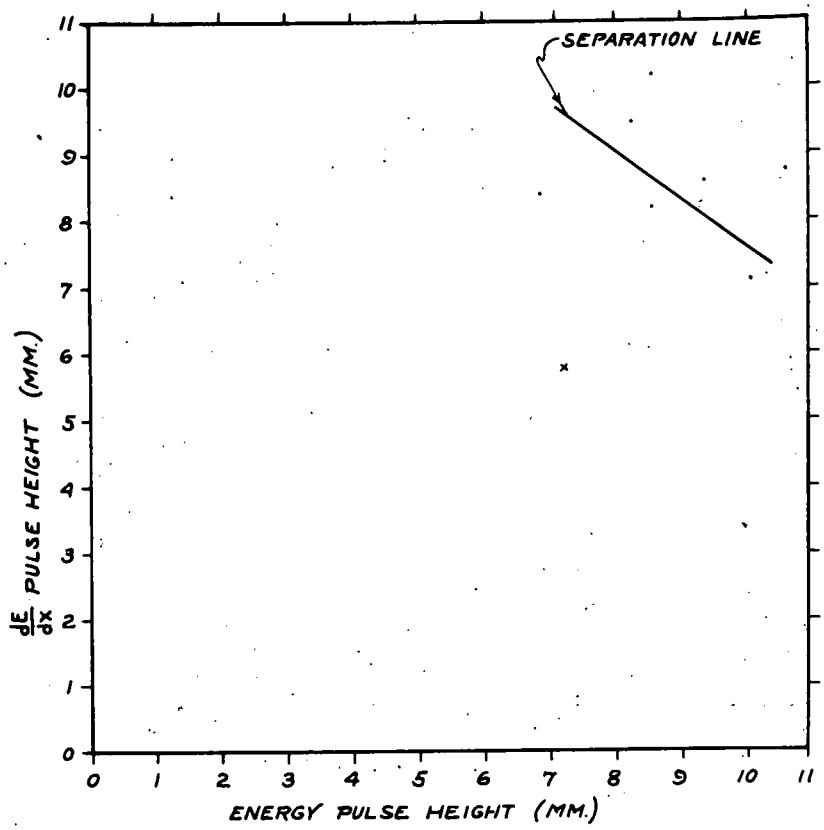

Fig. 24 — Final data for counting rate of H^3 using blank target. Data obtained in two integrated beam units.

He^3 fall in an island well separated from the expected slow-deuteron and proton background. One hundred and sixty-four counts were recorded in 10 integrated beam volts. It should be noted that several He^3 particles have the proper dE/dx, but have an energy pulse height lying below that to be expected from the resolution of the equipment. These are assumed to be He^3 particles that suffered an inelastic event in stopping in the energy detector. This argument is developed in the discussion of the H^3 data, where a calculation of this effect is required.

The blank-run data in Fig. 22 recorded three counts in 2.5 integrated volts. The ratio of the liquid-deuterium to blank counting rate, therefore, is of the order of 14 : 1. It is felt that this probably approximates the actual density ratio of liquid deuterium to gaseous deuterium in the target. It is possible, however, that He^3's of the proper energy may be created in the target window material by a pick-up mechanism in which a deuteron picks up a proton having a suitable internal momentum.

The H^3 data in Figure 23 do not resemble the anticipated results. Instead of having two well-defined areas of H^3 and fast deuterons, they show that deuterons of lower energy than those anticipated are being detected. By a process of elimination, it was determined that these deuterons did come from the target and did come down the channel. With the collimation used, however, they could not come down the channel in a direct path. It was finally determined that they represented deuterons that had scattered off one edge of the collimating slit at the entrance to the magnet. A further check of the geometry showed that deuterons might reach the detectors by such a process with energies down to approximately 120 Mev.

In order to separate these deuterons from the H^3, the resolution of the second and third detectors for deuterons of various energy was first determined from the deuteron calibration data. Figures 25 and 26 show typical resolution functions as determined by 200 random deuterons of 130 Mev. These resolution functions not only determine the width of the deuteron band, but locate accurately the center of the distribution on the dE/dx vs. energy plot for each calibration energy. In Fig. 27 the locus of the center of these distributions is shown.

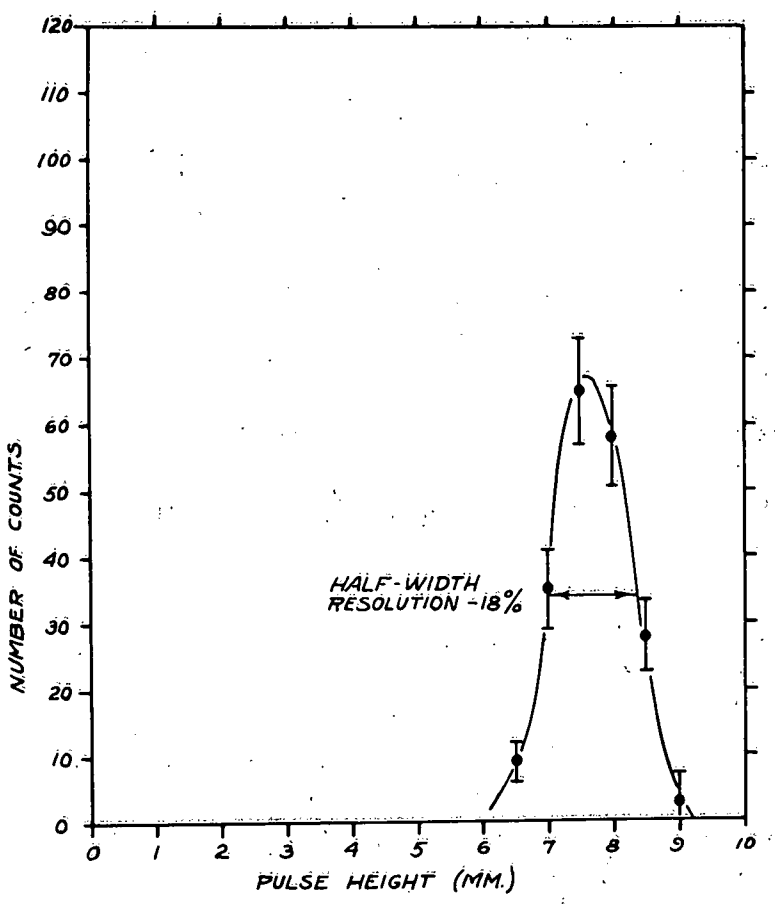

Fig. 25—Distribution in pulse height for deuterons of 130 Mev initial energy as measured by second detector.

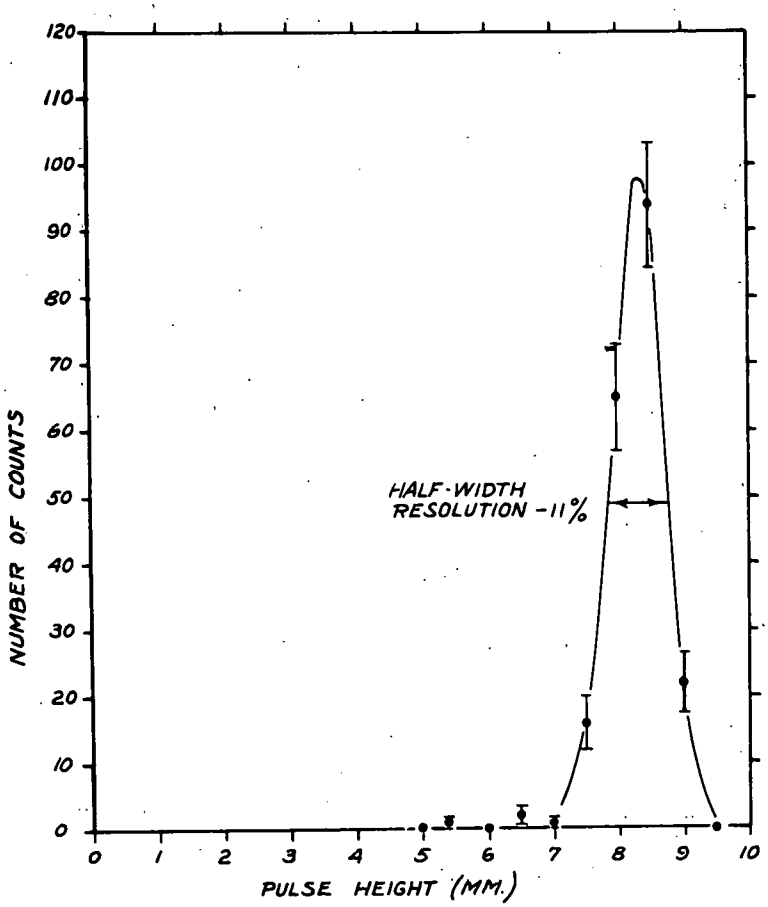

Fig. 26—Distribution in pulse height for deuterons of 130 Mev initial energy as measured by third detector.

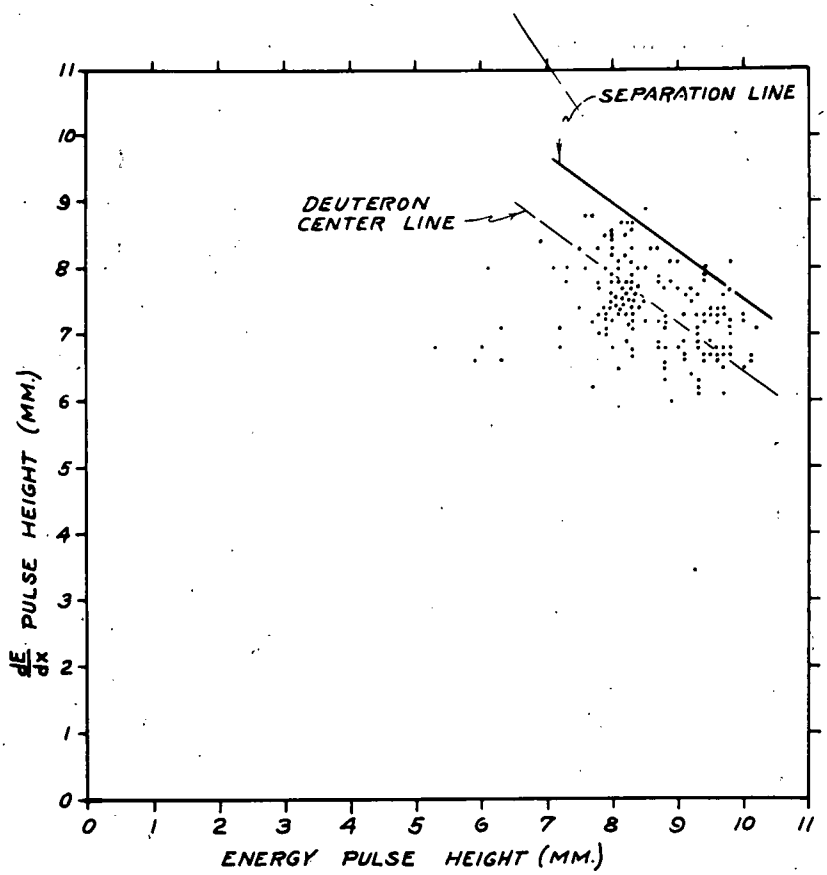

Fig. 27 — One hundred and sixty random pulses made by deuterons of various energies from 110 to 150 Mev. One curve shows locus of center of deuteron distribution. Other curve shows separation line between H^3 and deuterons.

(For the sake of illustration, there are also plotted the pulse heights of 160 random deuterons of various energies ranging from 110 Mev to 150 Mev.) A line was drawn parallel to this line that appeared to lie midway between the center of the deuteron distribution and the center of the triton distribution of Fig. 23. By superimposing this new separation line on the resolution plots, it was determined that from 2 to 3 percent of the deuterons would fall above this line. Assuming the detectors had the same resolution for H^3 as for deuterons, this would mean approximately 2 to 3 percent of the H^3 might fall below the line. This much was deemed satisfactory to effect a separation between the two. The points above the separation line in Fig. 23 were counted and found to be 129 for 10 volts of integrated beam. The blank-run data of Fig. 24 shows 4 counts in 2 volts.

Corrections

It was necessary at this point to introduce the only correction factors applied to the data. As mentioned previously, the H^3 and He^3 can suffer inelastic events in the detectors that affect their pulse heights. The most common event is a stripping off of one or two particles in a manner similar to the familiar deuteron stripping. In the event that such a process occurs before or in the dE/dx detector, the particle definitely is lost, since neither the dE/dx or the energy pulse is proper for a H^3 or He^3. By use of Crandall's data to compute the attenuation of H^3 and He^3 prior to entering the energy detector it was found that 7 percent of the H^3 and 1 percent of the He^3 were lost.

The effect of an inelastic event in the energy detector is impossible to predict rigorously. The most common event making up the inelastic cross section is the stripping of a single particle from the H^3 or He^3. Since the resultant deuterons, neutrons, or protons are less ionizing than the original particle, it is assumed that energy-pulse degrading takes place in all cases. The pulse degrading of the H^3 is greater than that of the He^3, since there is a greater probability of neutrons' carrying off energy with no ionization. Moreover, the probability of an inelastic event is approximately four times as great for the H^3 as for the He^3, since it will go through four times as much matter in stopping (assuming that the inelastic cross sections of the two are equal over the major portion of their range).

The probability of an event in which all the energy of a H^3 or He^3 would become unavailable for ionization seems quite small. It might occur if the proton of a H^3 suffered a knock-on collision with a neutron in which charge was exchanged. In this event the three neutrons would carry off the energy of the H^3 with little probability of further ionization. It might also occur if the proton were stripped from the H^3 by a nucleus in such a manner that the resulting excited nucleus produced little or no ionization. The possibility of an event in which a He^3 would fail to produce a substantial amount of ionization is hard to conceive.

Since the degraded He^3 particles are still readily separable from the background, it is apparent that no correction need be applied to the He^3 from this source. It is reasonable to assume, however, that a considerable number of the particles in Fig. 23 that fall in the category of deuterons are actually H^3 whose energy pulse has been degraded sufficiently to make them indistinguishable from deuterons. That this is a reasonable assumption can be further argued from the fact that the scattering of deuterons off the collimating slit can account only for detected deuterons of energies ranging down to about 120 Mev. It is felt that a majority of the particles in Fig. 23 whose dE/dx pulse was larger than about 8.0 on the ordinate scale were actually degraded H^3.

It is not necessary to make this assumption to get a rough correction factor for this effect. It was assumed that in three-quarters of the inelastic events, the energy of the H^3 was degraded sufficiently to either lose the count completely or to throw it into the deuteron band. Crandall's data were used to determine this correction factor. The correction factors are summarized in Table VII.

TABLE VII

Particle	Attenuation before or in dE/dx Detector	Degrading before or in Energy Detector	Total
H^3	1.07	1.13	1.21
He^3	1.01	1.00	1.01

Results

The final counting rates are summarized in Table VIII.

TABLE VIII

Particle	Corrected Deuterium Rate (counts/volt)	Corrected Blank Rate (counts/volt)	Difference Rate
H^3	15.6 ± 1.3	2.4 ± 1.1	13.2 ± 1.7
He^3	16.5 ± 1.3	1.2 ± 0.7	15.3 ± 1.5

The final ratio for the production of H^3 to He^3 at the CoM scattering angle of 30^o is 0.86 ± 0.14. The errors shown are the statistical deviations related to the number of counts constituting the original data. Within statistics, therefore, the production probabilities of He^3 and H^3 are equal. Although the correction factors are relatively small, they may introduce an uncertainty of the order of 5 percent. An additional 5 percent uncertainty is estimated for possible differences in angular resolution and other systematic errors.

Conclusions

The existence of charge symmetry would predict that the cross sections for the production of H^3 and He^3 would be the same. Unfortunately the inverse is not necessarily true. The cross sections might conceivably be equal at some specific angle in spite of an asymmetry in the nuclear forces. Moreover, the matter of degree must be considered. Since the cross sections cannot be calculated explicitly in terms of the n - n and p - p forces, it is not possible to say how much effect an asymmetry in the forces would have upon the cross sections. The following conclusion, however, seems justified: At low energy, charge symmetry is an established fact and the cross sections for the production of H^3 and He^3 from deuteron-deuteron collisions are equal (neglecting of course Coulomb and mass-difference effects). The fact that the cross sections are nearly equal at high energy supports the hypothesis of charge symmetry at high energy.

ACKNOWLEDGMENTS

It is a real pleasure to acknowledge my appreciation to Dr. Burton J. Moyer for his support during my graduate research under his direction. His support included not only guidance and advice throughout the course of the experiment, but also many late evenings at the cyclotron.

The author is particularly indebted to Drs. Kenneth Bandtel and Wilson Frank, who shared much of the onerous work of carrying out the cyclotron runs, and to Dr. Richard Madey, who led the development of the electronic equipment used. Thanks are due to the graduate students of Dr. Moyer's groups for their help in executing the cyclotron runs. Paul Nikonenko has made much of the electronic equipment used.

The successful operation of the liquid-deuterium target is in no mean part due to the work of Roscoe Byrnes and Robert Mathewson. Drs. Bludman and Heckrotte have helped in providing a theoretical approach to the experiment. James Vale and his cyclotron crew have been most co-operative in providing the means for doing the experiment.

This work was performed under the auspices of the Atomic Energy Commission.

APPENDIX

Small-Angle Scattering Correction

As charged particles pass through matter, they undergo a large number of small-angle deviations owing to Coulomb interaction with charges on the nuclei. These angular deviations can be treated statistically to give a probability distribution of angle or displacement for the particle; the distributions are usually gaussian in form and characterized by a mean square scattering angle or displacement. The most complete theoretical treatment are those of Rossi and Greisen[28] and Eyges.[29]

If only one of the $d + d \rightarrow H^3 + p$ products were being measured, the main effect of small-angle scattering would be to spread out the energy spectrum of the particles, since about as many particles would scatter into the detector as would scatter away from it. When two particles are being detected, however, the probability functions must be folded together, and the correction can become quite large. As previously mentioned, the proton detector in this experiment was chosen to subtend a considerably larger solid angle than the triton detector in order to keep these corrections small.

In the formulae shown below, the following notation is used: P is the relativistic momentum in Mev; β is the velocity of the particle in units of light; E_s is a combination of constants equal to 21.2 Mev. The thickness of scattering matter, t, is measured in radiation lengths. For greater utility, the mean square scattering angles or displacements are expressed in terms of their projections on a plane containing the particle's original direction.

The path of each particle requires three different scattering calculations. The first is due to scattering in the target. In this case the energy can be assumed constant and the mean square projected angle is given by

$$\left\langle \theta^2 \right\rangle_{\text{average}} = \frac{E_s^2 \quad t}{2 P^2 \beta^2}$$

The second calculation involves the scattering in the air path between the target and detector. Here again the energy can be assumed to be constant

and the mean square projected displacement is

$$\left\langle y^2 \right\rangle_{\text{average}} = \frac{E_s^2 \; t^3}{6 \; P^2 \; \beta^2}$$

The third calculation involves the scattering in the absorbers in front of the detectors. The calculations on this effect were based on the data of Millburn and Schecter[22]. The scattering effects were negligible compared to the other effects and were omitted.

The displacement due to air scattering can be expressed as an equivalent mean square scattering angle at the target. It can then be compounded with the first scattering angle to give a total equivalent mean scattering angle. If the angular limits of the detector are given by θ_1 and θ_2 as seen from the target, then a function $h(\theta)$ can be calculated and plotted giving the probability that a particle directed along θ before scattering will pass through the limits of the detector after scattering. Such functions can be calculated for both the proton and triton in both horizontal (or polar) and vertical (or azimuthal) directions. The horizontal plane is the plane containing the beam axis and the centers of the two detector systems. The net probability that both particles pass through their respective detectors is then proportional to $h_p(\theta_p) \cdot v_p(\phi_p) \cdot h_t(\theta_t) \cdot v_t(\phi_t)$ where θ is the polar angle, ϕ is the azimuthal angle, h is the horizontal probability and v is the vertical probability. Since both θ_p and θ_t, and ϕ_p and ϕ_t are correlated, the probability can be consolidated to $H(\theta) \cdot V(\phi)$. It is assumed at this point that the cross section did not vary violently over the face of the counter. It is then possible to integrate numerically the probability function over all possible angles of θ and ϕ, i.e., $\int H(\theta) \cdot V(\phi) \sin\theta \, d\theta \, d\phi$. When this integral is divided by the total solid angle of the defining detector, i.e., $\int \sin\theta \, d\theta \, d\phi$, the total probability of intercepting both particles is found. The numerical integration is facilitated by noting that $\int H(\theta) \cdot V(\phi) \sin\theta \, d\theta \, d\phi$ is equal to $\int H(\theta) \sin\theta \, d\theta \cdot \int V(\phi) \, d\phi$ and that $\sin\theta$ can be assumed constant over the counter. The small-angle scattering correction is the reciprocal of the interception probability.

REFERENCES

1. R. Serber, Phys. Rev. 72, 1008 (1947)
2. W. Heckrotte and S. Bludman. Private communication.
3. J. Allred, D. Phillips, and L. Rosen, Phys. Rev 82, 782 (1951)
4. H. Burrows, W. Gibson, and J. Rotblat, Proc. Roy. Soc. A-209, 489 (1951)
5. H. Leiter, F. Rodgers, and P. Kruger, Phys. Rev. 78, 663 (1950)
6. G. Hunter and H. Richards, Phys. Rev. 76, 1445 (1949)
7. K. Erickson, J. Fowler, and E. Stovall, Phys. Rev. 76, 1141 (1949)
8. J. Blair, G. Freier, E. Lampi, W. Sleator, and J. Williams, Phys. Rev. 74, 1599 (1948)
9. F. Ajzenburg and T. Lauritsen, Revs. Modern Phys. 24, 321 (1952)
10. J. M. Blatt and V. F Weisskopf, "Theoretical Nuclear Physics", New York, Wiley, 1952, p. 204
11. K. Watson and R. Stuart, Phys. Rev. 82, 738 (1951)
12. K. Allen, E. Almquist, J. Dewan, T. Pepper, and J. Sanders, Phys. Rev. 82, 262 (1951)
13. M. Stern, Experiments On Elastic Scattering of 190-Mev Deuterons By Protons, Thesis, University of California Radiation Laboratory, Report No. UCRL-1440, August, 1951
14. W. Powell, Physics Division Quarterly Report, University of California Radiation Laboratory, Report No. UCRL-1191, March 20, 1951
15. B. Youtz, Elastic and Inelastic Scattering of 90-Mev Neutrons by Deuterons, University of California Radiation Laboratory, Thesis, Report No. UCRL-2307, Aug. 13, 1953
16. W. Barkas and H. Wilson, Phys. Rev. 89, 758 (1953)
17. W. Frank, The Angular Distribution and Yield of the Process $p + d \rightarrow t + \pi^+$, Thesis, University of California Radiation Laboratory, Report No. UCRL-2292, May 18, 1953
18. R. L. Garwin, Rev. Sci. Instr. 21, 569 (1950)
19. R. L. Garwin, Rev. Sci. Instr. 23, 755 (1952)
20. H. Kallman and M. Furst, Phys. Rev. 81, 853 (1951)
21. W. Aron, B. Hoffman and F. Williams, Range Energy Curves, Report No. AECU-663 (Revised 1949)

22. G. Millburn and L. Schecter, Graphs of RMS Multiple Scattering Angle and Range Straggling For High Energy Charged Particles, University of California Radiation Laboratory, Report No. UCRL-2234, June 1, 1953

23. A. Kirschbaum, Nuclear Absorption Cross Section For High Energy Protons, Thesis, University of California Radiation Laboratory, Report No. UCRL-1967, October, 1952

24. W. Crandall, Private communication.

25. G. Chew and M. Goldberger, Phys. Rev. 77, 470 (1950)

26. W. Hess, Private communication.

27. L. Landau, J. Phys. (U.S.S.R.) 8, 201 (1944)

28. B. Rossi and K. Greison, Revs. Modern Phys. 13, 240 (1941)

29. L. Eyges, Phys. Rev. 74, 1534 (1948)